

Converting Post-Consumer Recycled Polyurethane Mattress Foam into Surface-Engineered Powders

Final Report

Primary Author: Clarissa Clifton

Sub Author: Hunaid Nulwala

RoCo®

December 2025

Table of Contents

ABSTRACT	3
BACKGROUND	4
FOAM COLLECTION & PROCESSING	5
MATERIAL CHARACTERIZATION	5
BULK PROPERTIES	5
THERMOGRAVIMETRIC ANALYSIS	6
HEAT FLOW ANALYSIS	10
CHEMICAL COMPOSITION ANALYSIS	10
APPLICATIONS TESTING	14
CEMENT ADDITIVE	14
<i>Sample Preparation</i>	14
<i>Bulk Property Analysis</i>	14
<i>Thermal Insulation Capabilities</i>	15
<i>Paint Adhesion</i>	16
<i>Salt Corrosion</i>	18
RIGID FOAM ADDITIVE	19
<i>Sample Preparation</i>	19
<i>Bulk Property Analysis</i>	19
NOISE DAMPENING	20
COMPRESSED FOAM SHEETS	21
<i>Sample Preparation</i>	21
<i>Sample Performance</i>	21
PRELIMINARY LIFE CYCLE ANALYSIS	22
CONCLUSIONS	23
REFERENCES	24
APPENDIX	25
APPENDIX A: PARTICLE SIZE DISTRIBUTION	25
APPENDIX B: DENSITY MEASUREMENTS FOR CEMENT SAMPLES WITH FOAM POWDER ADDITIVE	26
APPENDIX C: PAINT PEEL TEST COMPARISON IMAGES	27
APPENDIX D: SALT SPRAY EXPOSURE COMPARISON IMAGES	29
APPENDIX E: COMPRESSED FOAM SHEETS	41

Abstract

This report covers the development of a novel, proprietary grinding technology for pulverizing and functionalizing flexible polyurethane (PU) foams from recycled, post-consumer mattresses. Included are all stages from ideation, proof of concept, material characterization, scale up planning, and evaluation of possible applications.

While technologies exist for shredding rigid foams, there is no widely available technology for grinding flexible foams without relying on cryogenic processing. Roughly two billion pounds of flexible foam is discarded annually in the United States, most ending up in landfills or being incinerated [1]. Of this total, about 220 million pounds is recycled into carpet underlay, highlighting that the existing recycling methodologies don't allow for high-value application of the recycled material [1]. The technology developed by Roco® is designed to convert flexible foam waste into a powder with particle size and surface functionalization control, enabling tailoring as an additive for a wide variety of applications. These potential applications span many industries, including paints, batteries, polymer composites, adhesives, sealants, construction materials, and biotechnology.

Through an iterative design and testing procedure, we designed proprietary mechanical grinding equipment that can generate polyurethane powders with well controlled particle size in the sub-200-micron range, in a process that takes only minutes and can be carried out without the use of cryogenic temperatures.

The foam powder was characterized using brightfield microscopy, thermogravimetric analysis (TGA), differential scanning calorimetry (DSC), and Fourier transform infrared spectroscopy (FTIR). The characterization process focused on analyzing particle size and surface functionalization, which might have been influenced by the different system conditions applied during the foam to powder process. The three factors controlled were time, temperature, and incorporation of reactive gas during processing. In general, we found there are differences in PU foam powders produced across these different variables; these resultant differences varied in pronunciation for different permutations of the aforementioned factors. In summary, higher temperatures and reactive gases appear to have an interactive effect on the level of powder surface functionalization.

The powder was also tested as a functional additive across multiple applications, primarily in cement, rigid foam, and compressed foam sheets. These applications were assessed for impact of the foam additive on multiple material characteristics, such as thermal diffusivity, bulk density, noise modulation/dampening, and surface corrosion.

Background

Roughly 2.08 billion pounds of flexible polyurethane (PU) foam is used annually in the United States, about 50 percent of which is used in furniture and bedding [1]. Roughly 1.8 billion pounds of flexible foam used (or, 86.5 percent) is disposed of in landfills or by incineration [1]. Contributing to this total, more than 18 million mattresses are discarded every year in the United States, often ending up in landfills or incinerators [2]. This results not only in material going to landfill or incinerators but also lost opportunities to recover valuable materials. Flexible foam offers potential for upcycling into high-value products with several follow-on applications across a variety of industries.

Waste foams have traditionally been a challenge to recycle due to their toughness, elasticity, cross-linked structure, and thermal resistance. The primary outlet for scrap PU flexible foam today is carpet pad, which is produced by compressing and adhering mechanically shredded foam pieces into a high density rebond foam pad. However, as the volume of post-consumer foam for recycling increases, and demand for carpet rebond pad decreases, it is important to develop additional outlets for post-industrial and post-consumer flexible foam scrap.

Emerging chemical recycling methods, such as glycolysis or hydrolysis, are time and energy intensive, produce inconsistent products, and are inherently inefficient as they break the urethane bond to convert the polymer back to a mixture of amines and polyols. This makes them costly and less than ideal for commercial applications. Although there has been significant emphasis on chemical recycling to reclaim the polyols, these methods often require post-processing to separate complex mixtures of amines and polyols and yield materials that must be combined with large quantities of virgin materials to produce acceptable properties in finished polyurethane foams. Furthermore, these chemical recycling processes result in the loss of valuable components, such as the urethane group, which contains significant chemical functionality and potential value. This loss diminishes the overall material yield and does not capitalize on the material's full potential.

Recent studies have demonstrated the potential for mechanical and chemical approaches to reduce PU to fine powders that can retain or even gain functional groups (e.g., hydroxyl, amine), but these systems lack integrated thermal features, gas-phase reactivity control, and continuous process feedback [3], [4], [5]. These methods face challenges with limited scalability and application of recovered material due to long processing times and minimal control over the resultant particles. There is also some evidence in current literature for converting mattress foam into high-value products, such as graphite. Numerous studies have also been conducted to generate valuable end-products such as carbon precursors for battery manufacture and additives for cement composites [6]. However, these processes require large pyrolysis plants, which are energy-intensive and inefficient.

The system described in this report tackles these challenges with existing solutions via a grinding apparatus equipped with precise temperature and reactive gas control that results in fine size- and surface-chemistry tuned flexible foam particles. The surface modification of the foam powder allows for repurposing into high-performance polymer composites with potential utility for automotive and aerospace applications, durable specialty coatings, robust and flexible adhesives for manufacturing and medical fields, specialized lubricants for extreme conditions in machinery, scaffolding for biological tissue regeneration, and cutting-edge filtration media for water and gas purifications. This material can also be reincorporated into new foam materials resulting in product circularity. This approach not only diverts waste from landfills, but also creates significant economic opportunities by meeting the growing demand for sustainable, high-performance materials.

Foam Collection & Processing

All foam powder samples detailed in the following sections were produced using shredded post-consumer mattress foam provided by the Mattress Recycling Council (MRC) to RoCo®. Three factors were varied during the grinding process: processing time, system temperature, and gas infused during processing. The parameters assessed are shown in **Table 1**.

Table 1. Grinding System Parameters

Parameter (Factor)	Levels
Processing time	60, 180, and 360 seconds
System temperature	25, 60, 150, and 235°C
Gas perfused	N ₂ , CO ₂

This broad range of system condition permutations was only used during the material characterization phase of this project. For applications testing, system parameters were narrowed to 360 seconds, 60°C, and perfusion with either N₂ or CO₂.

Material Characterization

Bulk Properties

The bulk properties described here pertain only to foam powder samples used for applications testing (meaning, foam powder ground for 360 seconds at 60°C, perfused with either N₂ or CO₂). An example of the macroscopic and microscopic look of the foam powder is shown in **Figure 1**.

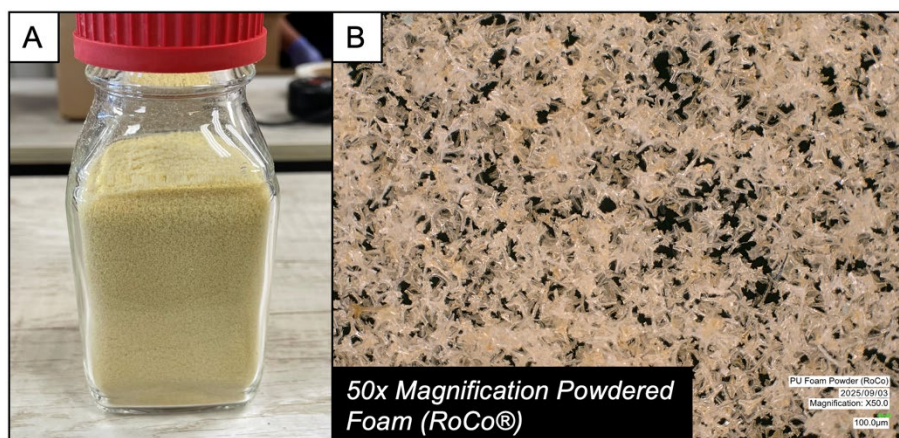


Figure 1: Macroscopic and Microscopic Images of Foam Powder. (A) shows ground foam as it appears to the naked eye. (B) shows foam powder under 50x magnification.

The two bulk properties analyzed were average bulk density of foam powder and average particle size. To determine

average bulk density of each powder type (foam processed under either N₂ or CO₂), the powder was scooped into a graduated cylinder. The graduated cylinder was then gently tapped repeatedly on a lab bench surface to eliminate any residual pockets of air until the volume marking remained stable for 2-3 subsequent taps. The mass and volume were then recorded, then density calculated (**Table 2**). The average bulk densities of the powders were 0.175 ± 0.0005 g/cc and 0.140 ± 0.0017 g/cc for powder processed under N₂ and CO₂, respectively.

Table 2. Foam Powder Bulk Density Measurements

Gas	Run	Mass (g)	Volume (mL)	Bulk Density (g/cc)	Avg. Density (g/cc)	Standard Error
CO ₂	1	7.16	50.0	0.1432	0.140	0.0023
	2	7.26	50.0	0.1452		
	3	1.37	10.0	0.1370		
	4	1.43	10.2	0.1402		
	5	1.24	9.4	0.1319		
N ₂	1	1.36	8.2	0.1659	0.175	0.0034
	2	1.79	10.6	0.1689		
	3	2.66	14.8	0.1797		
	4	2.51	14.2	0.1768		
	5	2.69	14.6	0.1842		

Results shown for foam powder ground for 360 seconds at 60°C, perfused with either CO₂ or N₂.

To measure the average particle size of each powder type, a thin layer of foam powder was sieved onto a glass dish then analyzed under 20x magnification (VHX-6000; Keyence Corporation; Osaka, Japan). A total of 100 measurements across the entire sample were taken using a 2-point measurement tool native to the microscope software. The two points were selected to measure the widest point of each measured particle. Using this method, the average particle sizes for foam processed under CO₂ and N₂ were determined to be 176 ± 2.1 microns and 167 ± 1.8 microns, respectively. Further details on the analysis of particle size distribution is shown in **Appendix A**.

Thermogravimetric Analysis

The analysis described here pertains to foam powder samples processed using the parameter permutations shown in **Table 1**. All samples were analyzed using thermogravimetric analysis (TGA) (Discovery TGA55; TA Instruments; New Castle, Delaware). Onset temperatures for each sample are shown in **Table 3**.

Table 3: Onset temperatures for PU foam samples.

Temp (°C)	Gas Type	Grind Time (s)	Onset 1 (°C)	Onset 2 (°C)
25	CO ₂	60	237.06	343.34
		180	246.61	338.93
		360	249.80	340.97
	N ₂	60	246.42	335.91
		180	245.47	341.29
		360	247.07	339.47
60	CO ₂	60	246.91	344.65
		180	248.30	342.45
		360	245.84	338.45
	N ₂	60	246.77	340.87
		180	244.78	341.94
		360	248.84	343.08
150	CO ₂	60	244.54	336.99
		180	250.66	345.84
		360	246.00	340.22
	N ₂	60	247.76	343.01
		180	248.75	343.33
		360	248.00	346.34
235	CO ₂	60	249.93	343.11
		180	248.57	340.81
		360	253.57	344.83
	N ₂	60	250.31	336.41
		180	247.88	329.56
		360	254.24	345.48

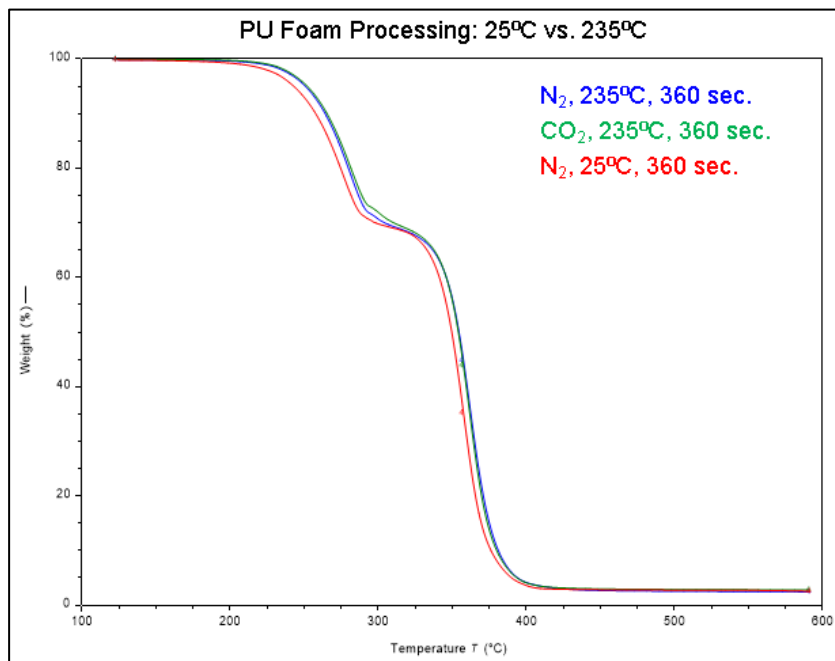


Figure 2: 25°C vs. 235°C. Image shows comparison of curves of samples processed at room temperature and at a high temperature. A clear shoulder can be seen forming in the curves of samples processed at 235°C near 295°C.

Figure 2 shows the comparison of weight percentage drop between foam processed under inert gas at room temperature and high-temperature processing conditions. This comparison makes obvious a definite shoulder in the curve as the TGA furnace temperature reaches roughly 295°C. While more pronounced in

the sample processed at 235°C under CO₂, this shoulder is also apparent in the sample processed under N₂ at the same temperature. This indicates that both system temperature and gas infused during grinding play a role in surface functionalization. However, their interaction is not clearly understood with current data collected.

After noticing this shoulder, we decided to obtain samples processed at 350°C, with an additional extreme case under CO₂ for 10 minutes (**Figure 3**). The goal was to see if grinding the foam at a temperature past the first onset temperature for all samples produced an even more noticeable effect. Numerical results are shown in **Table 4**. Note that while two onset temperatures are shown, the weight percentage steadily drops past the first onset temperature (i.e., a stable intermediate is not formed as the sample is heated). The CO₂, 10-minute sample had a single onset temperature at 347.96°C and a residual weight percentage of roughly 26 percent; this indicates some level of carbonization occurred during grinding of this sample. While this is interesting, we chose to not dedicate resources towards further characterizing this behavior.

Table 4: Onset temperatures of samples processed at 350°C.

Temp (°C)	Gas Type	Grind Time (s)	Onset 1 (°C)	Onset 2 (°C)
350	CO ₂	60	269.78	351.06
		180	266.86	353.12
		360	265.81	351.17
	N ₂	60	265.14	346.27
		180	276.42	344.56
		360	279.26	346.59

Converting Post-Consumer Recycled Polyurethane Mattress Foam into Surface-engineered Powders

Final Report (Contains no confidential information)

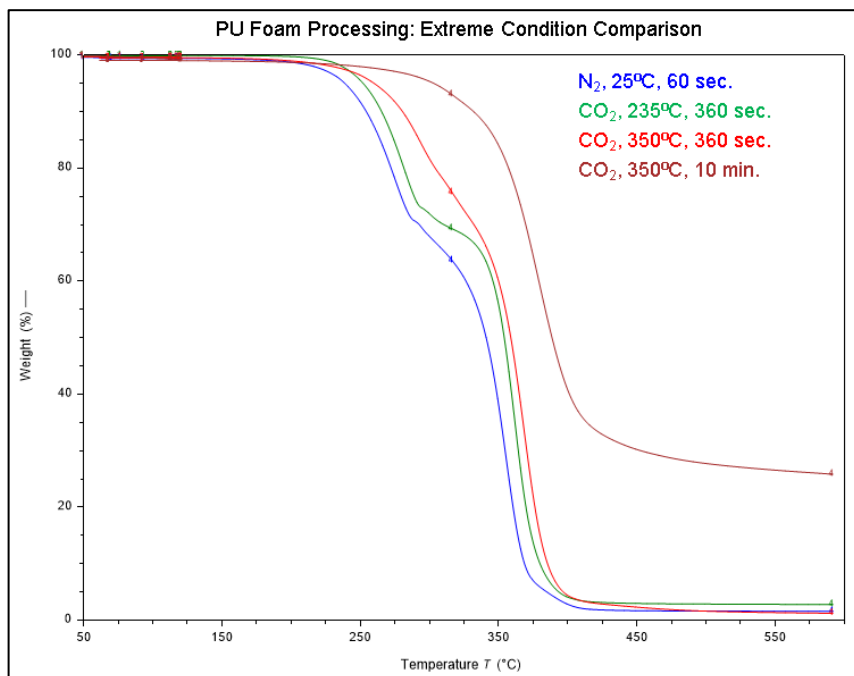


Figure 3: Extreme Case Comparison. Image shows comparison between samples processed at room temperature under inert gas and samples processed at higher temperatures under reactive gas.

Heat Flow Analysis

All samples were analyzed using Differential Scanning Calorimetry (DSC) (*Discovery DSC25; TA Instruments; New Castle, Delaware*). **Figure 4** shows an example overlay obtained during DSC analysis.

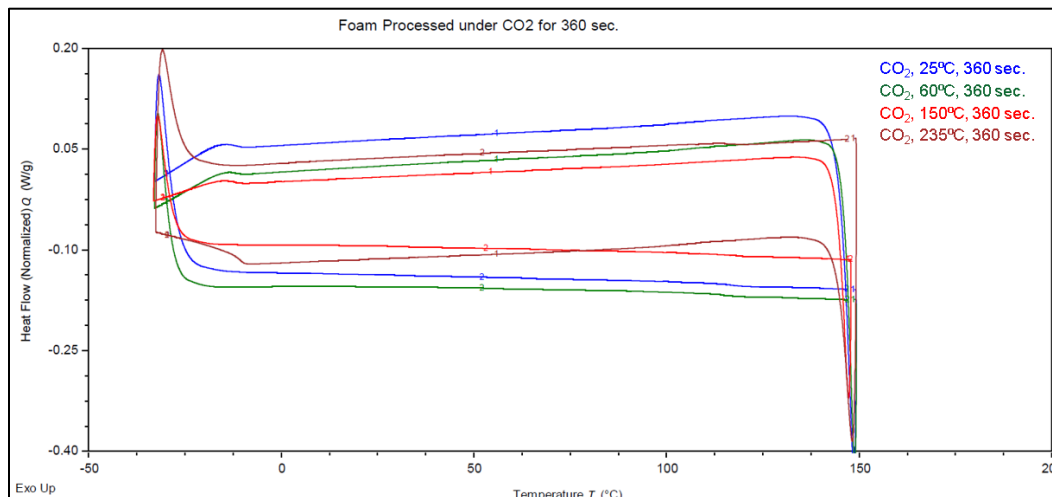


Figure 4: Overlay of Samples Processed under CO₂ across Various Temperatures.
Image shows an overlay plot of DSC data gathered for samples processed under CO₂ for 360 seconds across all controlled temperatures.

Of note is that there are certain sanity checks that cannot be easily explained by this data. For example, this overlay shows a glass transition temperature of roughly 110°C. This would indicate that the foam “feels” solid/inflexible at room temperature; however, the foam is incredibly flexible at room temperature, leading us to hypothesize that the true glass transition temperature should be much lower. Similar abnormalities are present across various response conditions. Therefore, further experimentation and characterization is required to elucidate the relationship between the factors and their effect on the material properties (such as the glass transition temperature).

Chemical Composition Analysis

All samples were analyzed using Fourier Transform Infrared Spectroscopy (FTIR) (*Nicolet™ iS™ 5 Spectrometer with iD5 ATR Accessory; ThermoFisher Scientific; Waltham, Massachusetts*). Two spectra were collected for each sample; these spectra were averaged to create one representative spectra for each sample.

Figure 5 shows the overlay of samples collected at room temperature under both CO₂ and N₂. There is relatively little difference between the two spectra, indicating that there is little to no difference in surface functionalization of the foam powder for samples processed at room temperature. However, once temperature increases, spectra for samples processed under CO₂ vs. N₂ show differences (**Figures 6-8**). This supports the previously described conclusion that both temperature and gas type play a role in surface functionalization (both independently and interactively). These FTIR results provide further insight that there is likely some threshold temperature, at which the samples must be ground, for the gas type to begin playing a role.

Converting Post-Consumer Recycled Polyurethane Mattress Foam into Surface-engineered Powders

Final Report (Contains no confidential information)

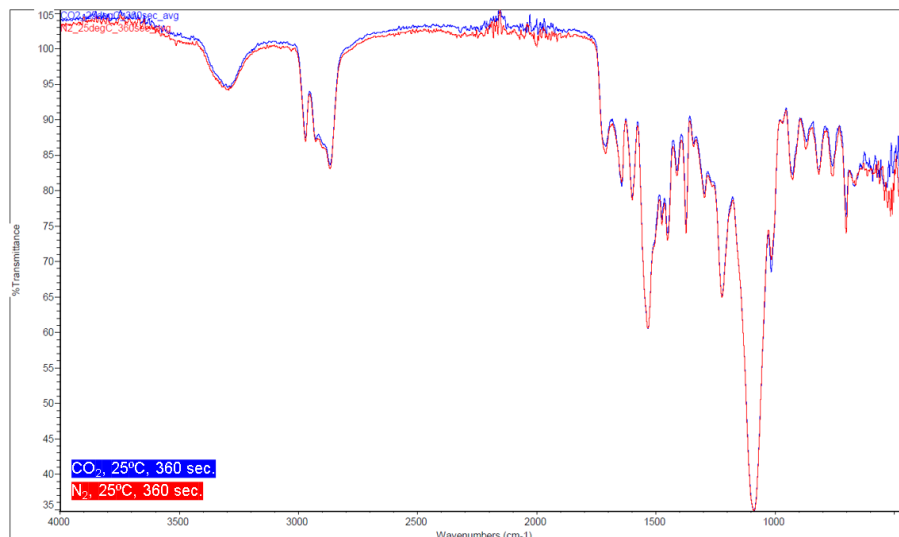


Figure 5: Room Temperature Comparison. Image shows overlay of samples processed at room temperature for 360 seconds.

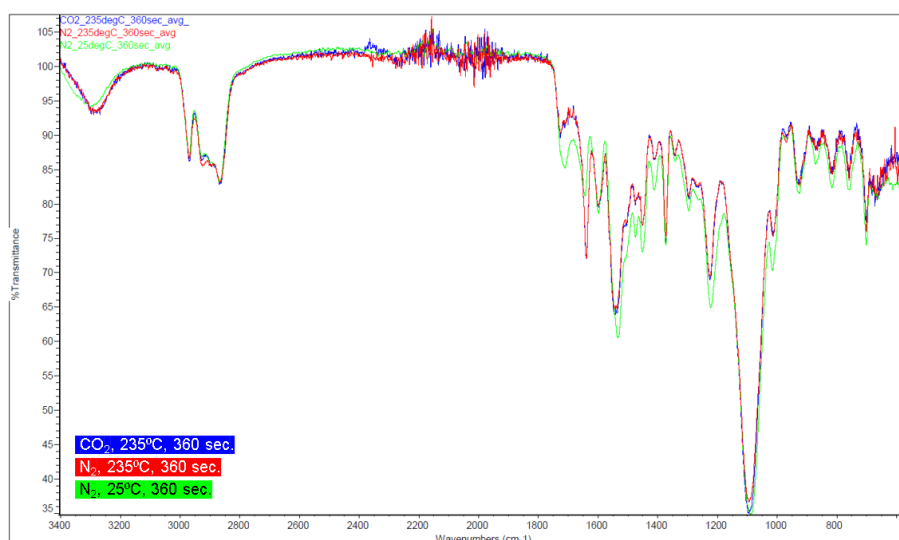


Figure 6: High Temperature and Reactive Gas Comparison. Image shows overlay of samples processed at 235°C under both N₂ and CO₂, showing differences from the sample processed at room temperature under N₂.

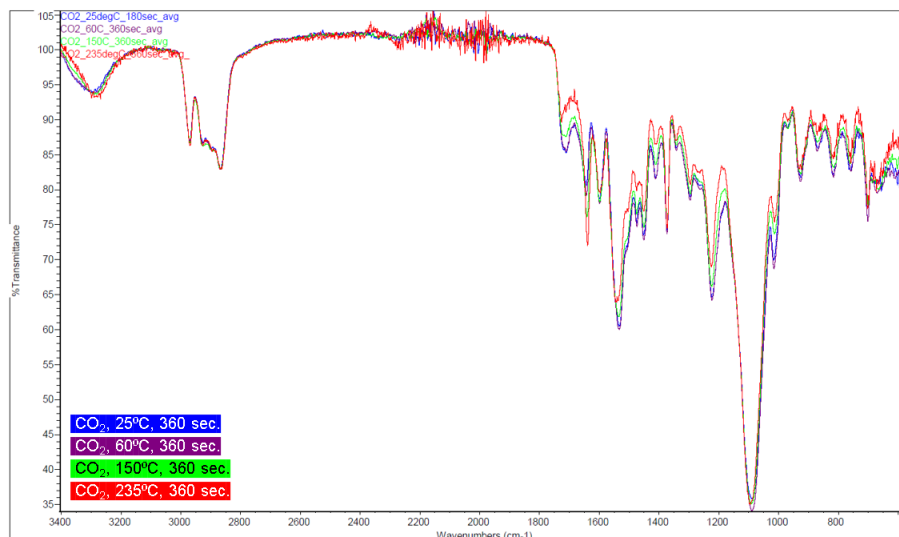


Figure 7: Samples Processed under CO₂ across all Temperatures. Image shows overlay of samples processed under CO₂ across all levels of temperature selected, showing differences as temperature increases.

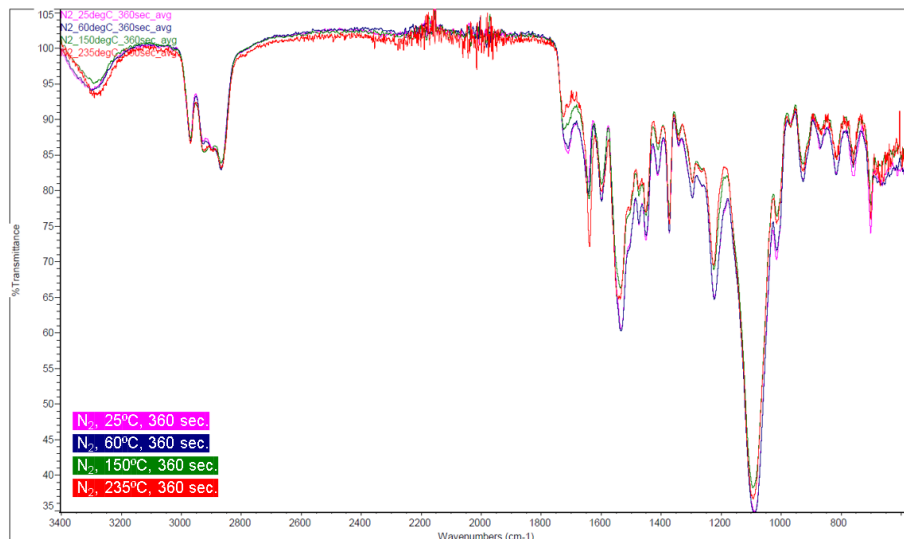


Figure 8: Samples Processed under N₂ across all Temperatures. Image shows overlay of samples processed under N₂ across all levels of temperature selected, showing differences as temperature increases.

More in-depth spectral analysis is described below; general trends hold true for all samples. Peak assignments for the analysis shown below are based on typical polyurethane functional groups [7], [8].

Room Temperature (25°C)

1. CO₂ vs. N₂:

- A slight increase in the peak at ~1090 cm⁻¹ was observed under CO₂ compared to N₂. This region is associated with C–O–C stretching in ether or ester linkages of PU [7].
- The peak at ~600 cm⁻¹, possibly related to out-of-plane bending of aromatic C–H or urethane linkages, was reduced under CO₂ compared to N₂.

- ##### **2. Interpretation:**
- The increase at 1090 cm⁻¹ suggests enhanced formation of ether/ester groups, possibly due to CO₂-induced surface oxidation. The reduction at 600 cm⁻¹ may indicate disruption of aromatic or urethane structures under CO₂.

Elevated Temperatures (25°C to 235°C) Under CO₂

1. Peak at ~3200 cm⁻¹:

- This broad peak, attributed to O–H stretching (e.g., from water, hydroxyl groups, or urethane N–H), sharpens with increasing temperature, particularly at 150°C and 235°C [8].
- **Interpretation:** Sharpening indicates loss of water or hydrogen-bonded hydroxyl groups, likely due to thermal dehydration or degradation of urethane linkages, forming a more defined signal for the N–H bonds.

2. Peak at ~1700 cm⁻¹:

- Assigned to C=O stretching in urethane or ester groups, this peak shows no significant change between 25°C and 60°C but diminishes significantly at 150°C and further at 235°C [7].
- **Interpretation:** The decrease suggests thermal degradation of urethane or ester carbonyls, possibly via decarboxylation or chain scission, accelerated under CO₂.

3. Peak at ~1650 cm⁻¹:

- Likely associated with amide C=O, this peak shows no major change at 25°C and 60°C but increases at 150°C and significantly at 235°C [8].
- **Interpretation:** The increase indicates formation of amide-like structures, possibly from thermal rearrangement or oxidative degradation under CO₂.

Comparison of CO₂ and N₂ at 235°C

1. Peak at ~3000 cm⁻¹:

- Under CO₂, this peak (likely C–H stretching in aliphatic or aromatic groups) decreases compared to N₂.
- **Interpretation:** CO₂ may promote oxidation or chain scission, reducing C–H content, while N₂ (inert) preserves these groups.

2. Peak at ~1650 cm⁻¹:

- Under CO₂, growth occurs at 235°C, with minor growth at 150°C. Under N₂, the peak shows less pronounced growth.
- **Interpretation:** CO₂ enhances formation of amide structures at high temperatures, possibly via oxidative pathways or interaction with CO₂ as a reactive gas.

3. Peak at ~3200 cm⁻¹:

- Under N₂, this peak decreases significantly at 150°C, indicating loss of O–H or N–H groups. Under CO₂, the peak broadens, suggesting retention of hydrogen-bonded species or formation of new hydroxyl-containing compounds.
- **Interpretation:** CO₂ may stabilize or form hydrogen-bonded structures (e.g., via carbamate formation), while N₂ allows thermal loss of these groups.

Proposed Chemical Mechanisms

1. Grinding-Induced Changes:

- Grinding under CO₂ may introduce mechanical stress and localized heating, leading to chain scission and exposure of reactive chain ends. CO₂, being mildly acidic, could react with urethane NH groups to form carbamates (R–NH–COOH) or promote oxidation. This explains the increase at 1000 cm⁻¹ (C–O–C) and reduction at 600 cm⁻¹ (disrupted urethane/aromatic groups).
- Under N₂, an inert atmosphere, mechanical degradation dominates without significant chemical interaction, preserving most functional groups.

2. Thermal Degradation Under CO₂:

- The sharpening of the 3200 cm⁻¹ peak suggests loss of water, possibly from dehydration of hydroxyl groups or urethane breakdown [9]. CO₂ may catalyze this by forming transient carbamates that decompose at higher temperatures.
- The decrease in the 1700 cm⁻¹ peak (C=O) at 150°C and 235°C indicates decarboxylation or cleavage of urethane/ester linkages, forming volatile CO₂ and amines [10].
- The increase in the 1650 cm⁻¹ peak suggests formation of C=C bonds (e.g., via elimination reactions) or amide-like structures from rearrangement of degraded urethane segments. CO₂'s oxidative potential at 235°C likely enhances these pathways compared to N₂.

3. CO₂ vs. N₂ at High Temperatures:

- CO₂'s reactivity at 235°C amplifies degradation, forming unsaturated or amide structures (1650 cm⁻¹) and reducing C–H content (3000 cm⁻¹). N₂, being inert, limits oxidative degradation, resulting in less pronounced changes.
- The broadening of the 3200 cm⁻¹ peak under CO₂ may result from CO₂ incorporation into the polymer (e.g., as carbamates) or retention of water/hydroxyl groups due to CO₂'s interaction with polar groups.

Applications Testing

Cement Additive

Sample Preparation

Samples for testing this application were prepared using commercially available “Rapid Set Cement All” cement powder. Samples were prepared by combining cement and foam powders at 5, 10, 15, and 20 percent by volume ratios for both N₂- and CO₂-processed foam powder variants. Negative control samples were prepared using only cement powder (with no foam additive).

Once the dry powder mixtures were prepared, water was added in a 4:1 powder-to-water ratio, as per manufacturer instructions (Rapid Set Cement All, CTS Cement Manufacturing Corp., Garden Grove, CA). The samples were initially mixed using a wooden popsicle stick to ensure no large clumps of powder were in the mixture; then subsequently mixed using a silicon mixing paddle attached to a drill motor for 30 seconds, clockwise, then 30 seconds counterclockwise, to ensure homogeneity of samples. Once homogeneous, the cement mixture was poured into silicone molds and left to cure on a lab benchtop 24 hours before demolding.

Bulk Property Analysis

Unsurprisingly, adding foam powder to cement impacts its density. To calculate this impact, two replicates were made of each permutation of processing gas and percent additive described above. The mass and physical dimensions were measured for each replicate, then average density for each condition was calculated based on these values. A summary of these results is shown in **Figure 9**. Generally, increased foam additive percentage resulted in decreased density of the cement sample; in all cases, the density decreased when compared to a negative control (cement with no foam additive). For the samples with added foam that was processed under N₂, there was an average density decrease of over 10 percent. Further details of these results are included in **Appendix B**.

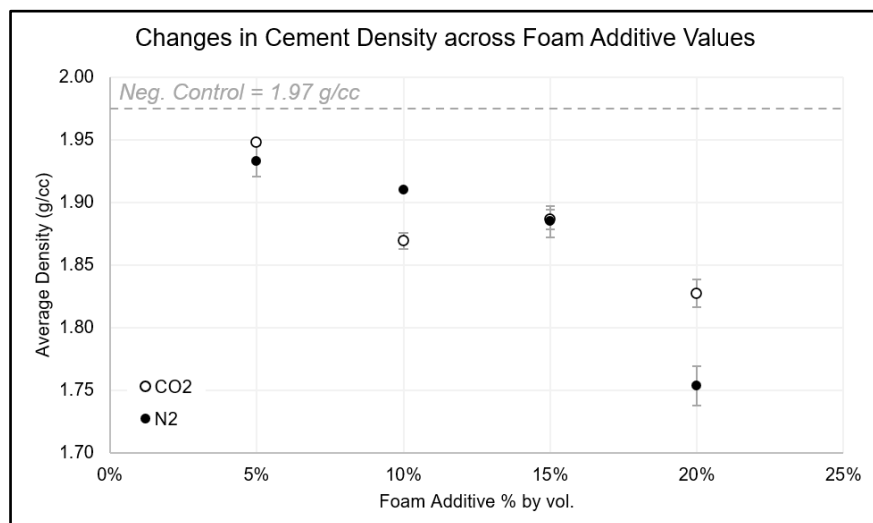


Figure 9: Foam Additive Impact on Cement Density. Figure shows general trend of decreased density as foam additive percentage increases. All conditions resulted in decreased density when compared to the negative control condition.

While not formally quantified during this phase, of note is the impact that foam additive had on the pouring behavior of the cement mixture. For foam powder processed under

both N₂ and CO₂, the cement mixture became noticeably more viscous as higher volume percentages of foam powder were added; this required more vigorous and frequent tapping on the silicone mold to eliminate air bubbles and ensure the cement evened out properly in the molds prior to curing.

Another property not formally quantified but notable was the foam additive's impact on drying time of the cement. While not incredibly pronounced at low additive percentages (5-10 percent), the cement samples appeared to dry more quickly than the negative control samples with any amount of foam additive. The most noticeable instance of this behavior was for samples with 20 percent foam processed under CO₂. For these samples, drying time appeared to reduce by roughly half. This property merits further exploration in follow-on research if cement additive applications become more relevant.

Thermal Insulation Capabilities

To get an idea of if/how thermal insulation capabilities were impacted by the PU foam additive, a thermal diffusivity test was conducted. This test was conducted by placing a J-type thermocouple to the center of a cement sample, then placing a roughly three-inch thick glass fiber insulating sheet on top of the thermocouple, recording initial temperature, placing the sample on top of a heated plate at a controlled temperature, then recording the time it took for the temperature of the thermocouple to rise by 10°C. This workflow is summarized in **Figure 10**.

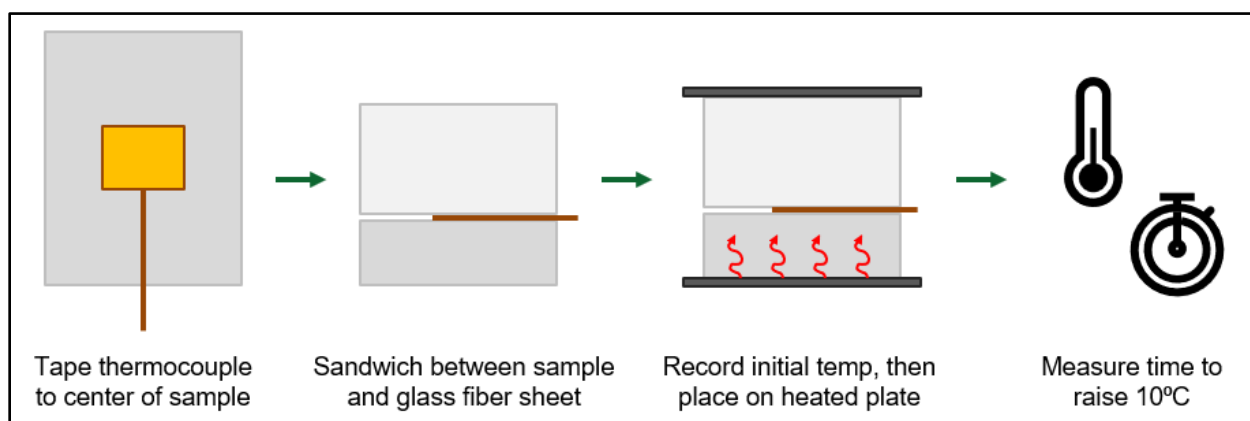


Figure 10: Thermal Diffusivity Experimental Workflow. Image shows steps taken during the testing of thermal diffusivity in cement samples with foam additive.

Figure 11 summarizes the results for the measured time to raise 10°C. Generally, there was no difference between foam additive types (processed under N₂ vs. CO₂). However, there was a difference when considering foam additive percentage. For samples with low additive ratios (5-10 percent), the time to raise 10°C decreased when compared to a negative control.

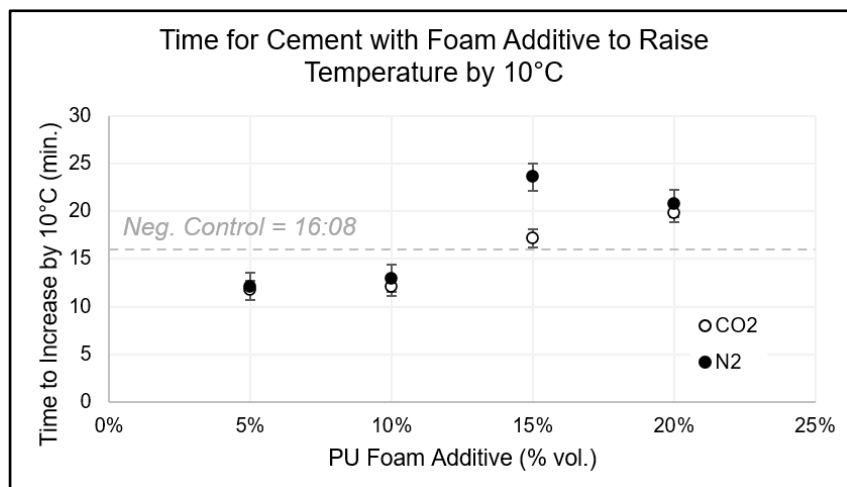


Figure 11: Time to Rise 10°C. The figure shows the time for cement samples with foam additives to rise by 10°C. The negative control had an average rising time of 16:08. Low foam additive ratios resulted in quicker times to rise temperature, while high foam additive ratios resulted in slower times to rise temperature.

Converting Post-Consumer Recycled Polyurethane Mattress Foam into Surface-engineered Powders

Final Report (Contains no confidential information)

For samples with high additive ratios (15-20 percent), the time increased compared to a negative control. These values were used to estimate thermal diffusivity using the following equation:

$$\alpha = \frac{L^2}{\pi^2 t}$$

Where α = thermal diffusivity (mm²/s)

L = sample thickness (mm)

t = time for temperature to rise 10°C (sec)

The values indicate that low foam additive percentages result in increased thermal diffusivity of the cement, meaning heat transfers more quickly through it. High foam additive percentages, however, resulted in lower thermal diffusivity, meaning heat transfers more slowly through the samples. The calculated values are summarized in **Table 5**.

The Cement All data sheet indicates the cured cement samples should have a density of 1.995 g/cc, which is slightly higher than our empirical value (1.975 g/cc) [11].

Table 5. Thermal Diffusivity Summary

Condition		Thermal Diffusivity (mm ² /s)
Negative Control		0.0440
CO ₂	5%	0.0509
	10%	0.0458
	15%	0.0329
	20%	0.0298
N ₂	5%	0.0571
	10%	0.0451
	15%	0.0236
	20%	0.0274

Lower density indicates more air in a sample, which is a poor heat conductor; it follows that the more air in a sample, the worse it would be at diffusing heat across its mass. At lower foam additive ratios (5-10 percent), the foam is likely serving primarily to create air pockets between cement particles. However, once a critical ratio is hit (somewhere between 10-15 percent additive ratio), it's likely that the foam particles are ubiquitous enough to interlock with each other. This would explain the dual action of lowered density and decreased thermal diffusivity compared to negative control and higher loading percentages. More thorough analysis is required to substantiate this hypothesis, however. Whatever the explanation, our results indicate the foam powder additive has promise in applications targeting thermal property modification in cement/mortar.

Paint Adhesion

To assess feasibility in interior cement markets, a test was performed to determine if/how the PU foam additive impacted paint adhesion to a cement surface (e.g., for use as an additive in interior cement flooring that may increase adhesion of floor coatings). This test was performed using a standard tape peel test [12]. A summary of this workflow is shown in **Figure 12**.

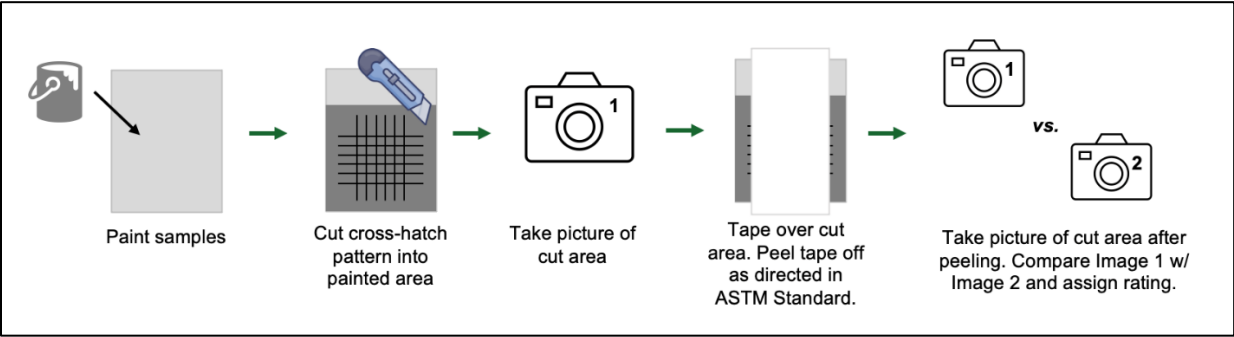


Figure 12: Paint Adhesion Test Experimental Workflow. Image shows testing procedure outlined in ASTM Standard D3359-09 for paint adhesion test on surface of cement samples with foam additive.

The tape peel test uses a rating system (0B-5B) to indicate the level of adhesion; **Table 6** summarizes the standard ranges, as well as each condition's rating. **Figure 13** shows sample comparison images. All comparison images are included in **Appendix C**.

Table 6. Paint Peel Test Ratings

Condition		Rating	Key	
Negative Control		3B	5B	0% loss
CO ₂	5%	4B	4B	<5%
	10%	3B	3B	5-15%
	15%	4B	2B	15-35%
	20%	3B	1B	35-65%
N ₂	5%	3B	0B	>65%
	10%	4B		
	15%	4B		
	20%	4B		

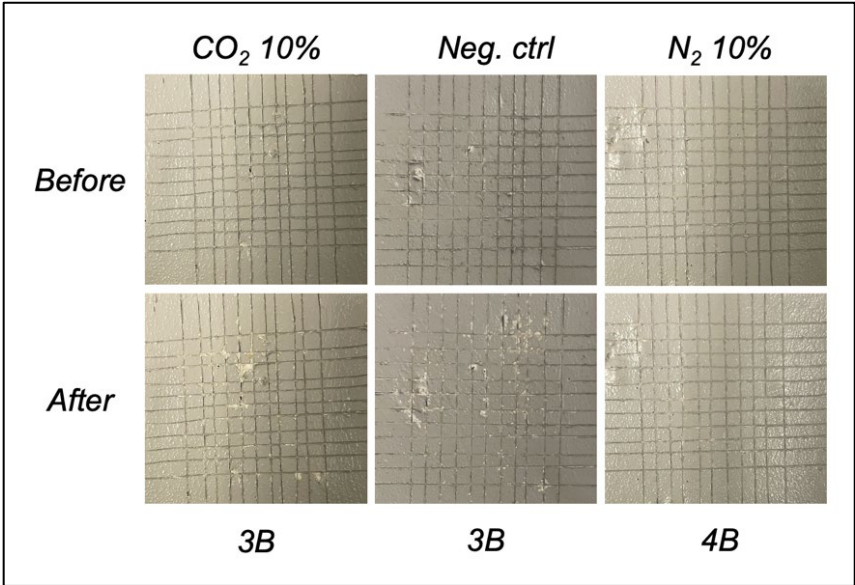


Figure 13: Sample Peel Test Comparison. Image shows comparison of before and after images taken to rate the samples' surface adhesion capabilities.

While there is slight improvement from negative control in a few of the samples, there is no clear trend that either foam additive is causing an impact (either positive or negative) on surface coating adhesion to the samples compared to the control. As such, these preliminary results don't

indicate there is much impact on paint/surface coating adhesion due to addition of our powdered foam additive. Possible confounding causes could be type of paint used and surface preparation of each sample (i.e., samples were not sanded or otherwise primed prior to painting); however, even with these confounding variables considered, we do not feel it is advantageous to continue research into coating adhesion improvement qualities of our foam additive at this time.

Salt Corrosion

Another possible application for the foam powder is as an additive to non-structural/non-load-bearing concrete (e.g., sidewalks, parking lots, etc.). For these uses, especially in the Northeast US region, the concrete will be exposed to salt for multiple months at a time. To assess the impact (if any) on salt corrosion resistance with our foam additive included, a salt spray test was performed according to an adaptation of ASTM Standard B117-11. A summary of the workflow conducted is shown in **Figure 14**.

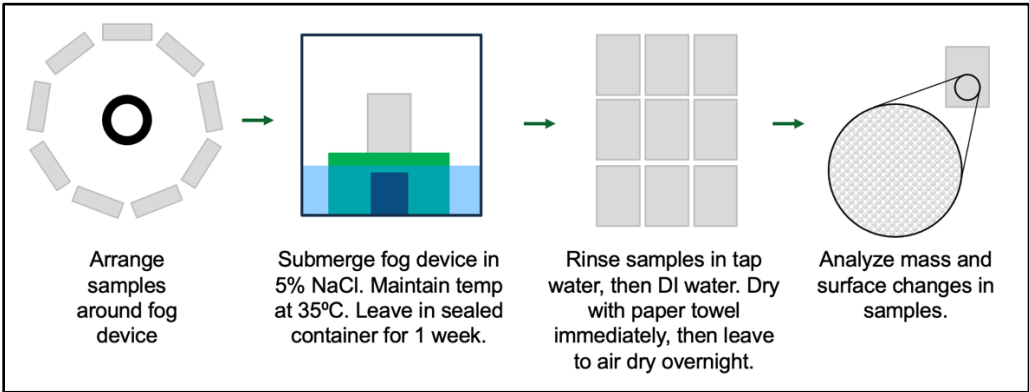


Figure 14: Salt Corrosion Test Experimental Workflow. Image shows testing procedure for salt corrosion test for cement samples with foam additive.

Images were taken under magnification before and after the salt spray test of each sample in five locations: one on each corner, and another in the center of the sample. Example images are shown in **Figure 15**. Additional images are included in **Appendix D**.

		Center	Bottom Right
N ₂ 10%	Before		
	After		

Figure 15: Sample Comparison Before and After Salt Spray Test. Image shows before and after salt spray test comparison of samples with 10% by vol. foam powder additive that was processed under N₂. Slight pitting can be seen in the bottom right location after exposure to salt.

All samples with foam powder additive processed under N₂ showed increased surface roughness at both bottom corners of each sample when compared to a negative control. This roughness indicates that these samples would show more drastic pitting/corrosion if exposed to salt for a longer duration (weeks to months). Samples that included foam powder processed under CO₂ did not show increased surface roughness but did show slight discoloration around the edges of each sample. Further characterization is needed to determine if the CO₂-processed foam powder has any other notable impacts under salt exposure, but these results indicate that N₂-processed powder should be ruled out for this application, as these samples appear to have accelerated surface corrosion when exposed to salt.

Rigid Foam Additive

Sample Preparation

Samples for this application were prepared using a commercially available rigid marine foam system with two parts: polyol and isocyanate. Samples were prepared by mixing foam powder with the polyol component of the foam system in 5, 10, 20, and 40 percent by weight ratios. Our ground foam powder was mixed with the polyol for 3 minutes using a silicone mixing paddle attached to a drill motor to ensure homogeneity. This polyol mixture was then combined with the isocyanate component of the foam system in a 1:1 ratio, as per manufacturer instructions. Once mixed, the foam was left in a fume hood for 24 hours to cure fully.

Bulk Property Analysis

The average density of all rigid foams with additive ratios at or below 20 percent by volume was lower than a negative control. **Figure 12** shows the comparison of all collected values. Of interest is that these samples also appeared qualitatively stiffer than the negative control. This indicates that increased stiffnesses are achievable at lower densities when including our foam additive, when compared to rigid foams with no additives. More quantitative data is required to confirm this hypothesis.

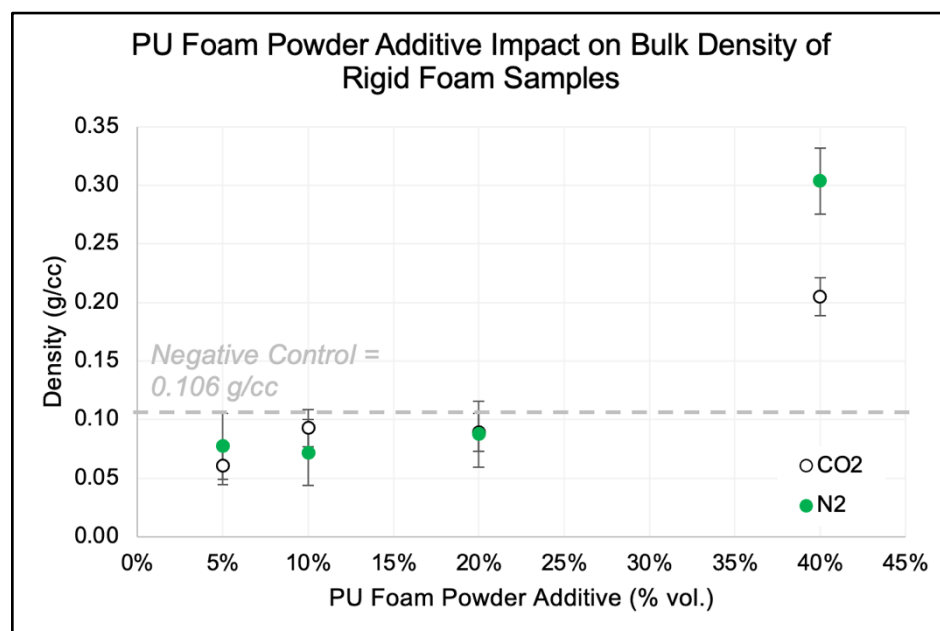


Figure 12: Powder Additive Impact on Rigid Foam Bulk Density. Image shows average densities of multiple rigid foam samples with powder foam additive ratios ranging from 5 to 40 percent by volume. All ratios other than 40 percent by volume were less dense than the negative control.

Noise Dampening

When considering noise dampening, there are two major modes of conduction to consider: airborne noise and impact noise. Airborne noise encompasses things like rain, music, and sirens. Impact noise includes “road noise” caused by the car vibrating against the road at high speeds and engine noise. We believe there are interesting applications for potential noise dampening in the automotive industry, specifically in the noise, vibration, and hum applications for electric vehicles.

We conducted an impact sound test using a ball bearing drop apparatus. A plastic box was 3D-printed and lined with foam (*Printer: Bambu Lab X1 Carbon; Filament: PLA Basic; Bambu Lab; Shenzhen, China*). Then, a microphone was placed inside the box. A plastic pipe was lined up over the center of the lid of the box, then a ball bearing was dropped from the top of the pipe to impact the box lid. The impact sound intensity and frequency were recorded by the microphone. This was repeated for a negative control, 5 percent by volume additive for both N₂- and CO₂-processed foam powder, and 10 percent by volume additive for CO₂-processed foam powder. Results for both intensity and frequency are shown in **Figure 13**.

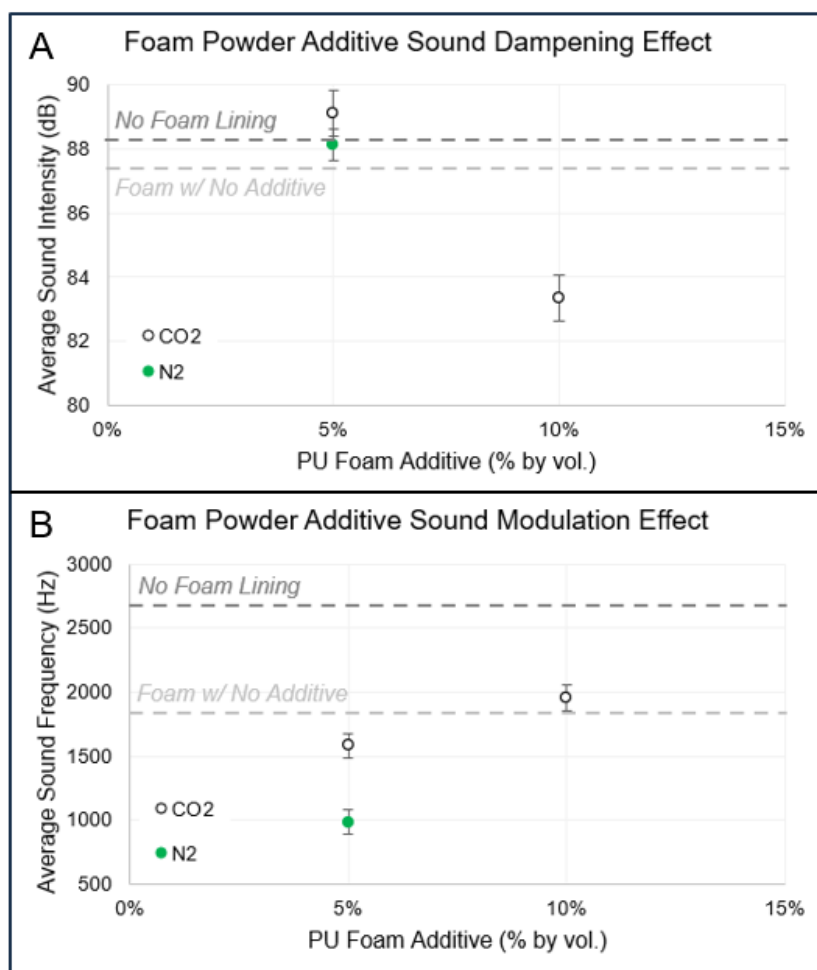


Figure 13: Dampening and Modulation Effects on Foam Samples with PU Powder Additive. (A) shows sound dampening effect on foam samples with additive. (B) shows sound frequency modulation effect on foam samples with additive.

Regarding dampening (sound intensity), it appears that neither sample with 5 percent by volume additive ratio caused noticeable sound dampening. The sample with 10 percent additive ratio caused noticeable sound dampening, but only by a few decibels. However, all foam samples caused significant frequency modulation (reduction) compared to the unlined plastic box. This indicates that while dampening may not occur at significant levels, high-frequency impact noise can be modulated to low-frequency noise. Current efforts are underway to better characterize this performance metric of rigid foam samples created with our foam powder

additive. We have built a noise isolation box with a slot to place foam samples directly between a speaker generating known frequency and volume sounds and a microphone. Recorded audio

files will be analyzed to determine foam additive impact on both recorded decibel levels and recorded noise frequencies.

Compressed Foam Sheets

Sample Preparation

Each compressed sheet was made using only foam powder, prepared as described in **Foam Collection & Processing**. Sheets were made by compressing 3 grams of foam powder at room temperature using a machine press. Sheets were prepared using both CO₂- and N₂-processed foam powder under compression forces of 2500, 5000, 10000, and 20,000 psi, with a dwell time of 15 seconds. One sample was made using CO₂-processed foam powder with a 20,000-psi compressive force and a dwell time of 2 minutes.

Sample Performance

For samples compressed under 2500 and 5000 psi, the sheets broke apart immediately once light pressure was applied by hand. When the force was increased to 10- and 20 thousand pounds-force, small pieces of the foam sheets stayed together after light pressure was applied, but these pieces had to be handled gently to avoid further damage. Generally, CO₂-processed foam powder sheets kept their structural integrity better than their N₂-processed counterparts. This is likely due to the surface functionalization introduced during grinding.

Figure 14 shows one of the samples directly after compression and after the sheet broke into pieces. **Figure 15** shows the microscopic interlocking of foam powder particles. Additional images can be found in **Appendix E**.

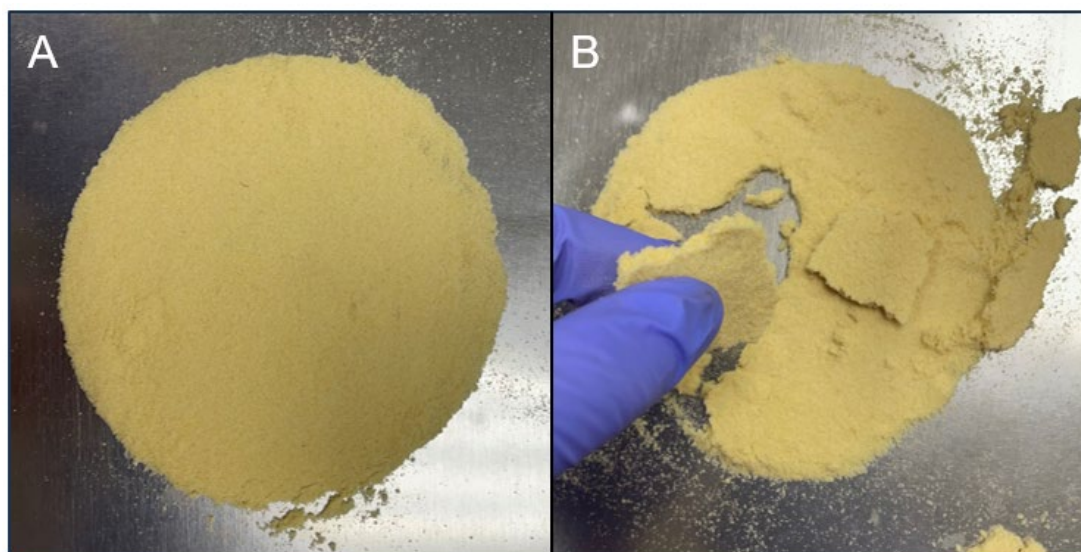


Figure 14: Compressed Foam Sheets. (A) shows sample immediately after compression. (B) shows sample after light pressure was applied by hand. Small pieces of the sheet maintain their integrity, but the sheet as a whole is structurally compromised.



Figure 15: Compressed PU Foam Powder Sheets (50x). Image shows two samples of compressed foam powder: 2500 pounds-force (left) and 20,000 pounds-force (right). While there is interlocking of foam pieces in the sample on the left, there is noticeably more in the sample on the right, which was compressed at a higher compressive force.

However, no samples kept their structural integrity after light hand pressure was applied. For compression into foam sheets to be successful, it's likely some binder, heat, or combination of both would need to be applied. This is likely worth exploring for future adjacency moves into applications such as filtration.

Preliminary Life Cycle Analysis

A preliminary life cycle impact assessment (LCIA) for the grinding process was conducted using openLCA software. Our analysis focused on 1 kg of processed foam, with electricity sourced from Duke Energy Progress East. We employed the TRACI 2.1 impact method for the assessment, using background data from the USLCI database and applying normalization and weighting via the US 2008 TRACI 2.1 set.

Interestingly, even when accounting for electricity consumption, the results showed no measurable environmental impact across all TRACI categories. This suggests that the grinding process, as modeled, is environmentally benign and does not significantly contribute to emissions or resource depletion. Thus, we can confidently conclude that flexible foam grinding is a low-impact process that effectively diverts waste into useful products. The use of nitrogen and carbon dioxide during grinding was deliberately ignored due to difficulty identifying reliable values to incorporate into the model.

To gain a sense of where our process stands in comparison to traditional methods for foaming (i.e., making foam from virgin precursor materials), we compared our values to a cradle-to-grave analysis report from Franklin Associates [13]. This study evaluates the environmental impacts of producing polyether polyol only, meaning the isocyanate portion is not accounted for. This report follows ISO 14040/14044-compliant LCA using TRACI 2.1 and IPCC 2013 characterization factors. The key findings of the study are summarized below, while a comparison to our flexible foam grinding method is shown in **Table 7**:

1. Energy Demand: 87.8 GJ per 1,000 kg, with 99.1% from non-renewable sources
2. Global Warming Potential: 3,205 kg CO₂ eq per 1,000 kg, with 96% from upstream materials
3. Solid Waste: 125 kg total, with 95% from raw material production per 1000 kg of polyol
4. Water Consumption: 19,692 liters, mostly from upstream processes per 1000 kg of polyol
5. Main Contributors: Propylene oxide production dominates impacts across all categories

Table 7. Polyol Production vs. RoCo®'s Flexible Foam Processing

Factor	Polyether Polyol Production	RoCo®'s Proprietary Flexible Foam Processing
Scope	Cradle-to-grave	Gate-to-gate (processing only)
Energy use	High (87.8 GJ/1,000 kg)	Very low (e.g., 0.15 kWh/kg)
Global warming potential	High (3,205 kg CO ₂ eq/1,000 kg)	Negligible (0 kg CO ₂ eq reported)
Solid waste	Significant (125 kg/1,000 kg)	Minimal (mostly packaging waste)
Water consumption	High (19,692 liters/1,000 kg)	None
Main impact drivers	Raw material synthesis (e.g., propylene oxide)	Electricity use
Software & databases	openLCA, USLCl, ecoinvent, GREET	openLCA, USLCl, TRACI 2.1

Given the above comparisons, we conclude that the PU processing, as modeled, shows negligible environmental impact, especially when compared to the polyether polyol production, which is energy-intensive and emissions-heavy due to its reliance on fossil-based feedstocks and complex chemical synthesis. This contrast underscores the environmental benefit of recycling PU foam through mechanical grinding (such as through our developed process/technology) rather than producing virgin polyol from petrochemicals.

However, an important caveat of this conclusion is that this comparison may not be the relevant one to make for some applications. If the foam powder is used as an additive in foam products, such as spray foams, acoustic paneling, or flexible foam products, whose goal is to be more circular, then this comparison to virgin materials holds true. However, if our foam powder is to be used in other polymer materials, a more relevant comparison would be incumbent fillers in those fields (such as calcium carbonate). Nevertheless, our preliminary analysis shows that the production process of the foam powder developed by RoCo® uses very little energy, produces negligible greenhouse gas emissions, solid waste, or water usage during manufacturing.

Conclusions

The proprietary processing technology developed over the course of this project shows promise for further development. We are currently able to achieve control of the foam powder's particle size, resulting in about a 10x increase in bulk density from the recycled post-consumer foam upon converting to foam powder. While further characterization is still needed to fully understand the interactive effect on the foam powder between increased system temperature and type of gas perfused, we have shown evidence consistent with functionalization of the foam powder during the grinding process. We intentionally chose to scale back this characterization to focus on applications testing to identify potential target markets.

When choosing an initial primary target market, we must balance the most interesting material characteristics we've uncovered thus far with the shortest route to a sale. We believe the best choice is to focus on use of our foam powder as an additive in rigid foam. The most interesting characteristics caused by our foam additive in rigid foam are noise modulation and increased rigidity at lower densities. Considering this, we believe the best primary target market is functional additives in non-structural construction materials (e.g., rigid foam slabs in building sidings, garage doors, front doors, acoustic panels, etc.). This market represents a \$1.5 billion addressable market opportunity in the United States, and a \$5 billion global opportunity [14].

Current efforts are ongoing to validate data described in this report, as well as to perform market validation for the selected target market. We are also working to build relationships with top manufacturers, customers, brand owners, and industry partners in the foam industry to ensure successful market entry for our product.

References

- [1] C. Liang *et al.*, “Material Flows of Polyurethane in the United States,” *Environ. Sci. Technol.*, vol. 55, no. 20, pp. 14215–14224, Oct. 2021, doi: 10.1021/acs.est.1c03654.
- [2] “Why Recycle,” Mattress Recycling Council | Recycling Programs in California, Connecticut & Rhode Island. Accessed: Feb. 25, 2025. [Online]. Available: <https://mattressrecyclingcouncil.org/why-recycle/>
- [3] C. Pei, J. Zong, S. Han, B. Li, and B. Wang, “Ni-Catalyzed Direct Carboxylation of an Unactivated C-H Bond with CO₂,” *Org. Lett.*, vol. 22, no. 17, pp. 6897–6902, Sept. 2020, doi: 10.1021/acs.orglett.0c02429.
- [4] L. Guo *et al.*, “Recycling of Flexible Polyurethane Foams by Regrinding Scraps into Powder to Replace Polyol for Re-Foaming,” *Materials*, vol. 15, no. 17, p. 6047, Sept. 2022, doi: 10.3390/ma15176047.
- [5] L. Guo *et al.*, “Mechanochemical Recycling of Flexible Polyurethane Foam Scraps for Quantitative Replacement of Polyol Using Wedge-Block-Reinforced Extruder,” *Polymers*, vol. 16, no. 12, p. 1633, June 2024, doi: 10.3390/polym16121633.
- [6] “High-Performance Carbon from Recycled Mattress for Supercapacitor Devices | SpringerLink.” Accessed: Feb. 26, 2025. [Online]. Available: https://link.springer.com/chapter/10.1007/978-981-99-9931-6_16
- [7] G. Socrates, “Infrared and Raman Characteristic Group Frequencies: Tables and Charts, 3rd Edition | Wiley,” Wiley.com. Accessed: Oct. 17, 2025. [Online]. Available: <https://www.wiley.com/en-us/Infrared+and+Raman+Characteristic+Group+Frequencies%3A+Tables+and+Charts%2C+3rd+Edition-p-9780470093078>
- [8] R. M. Silverstein, F. X. Webster, D. J. Kiemle, and D. L. Bryce, “Spectrometric Identification of Organic Compounds, 8th Edition | Wiley,” Wiley.com. Accessed: Oct. 17, 2025. [Online]. Available: <https://www.wiley.com/en-us/Spectrometric+Identification+of+Organic+Compounds%2C+8th+Edition-p-9780470616376>
- [9] P. Z, Z. Z, F. J, and M. W, “Thermal degradation of segmented polyurethanes,” Jan. 1994, doi: 10.1002/app.1994.070510615.
- [10] D. Allan, J. Daly, and J. J. Liggat, “Thermal volatilisation analysis of TDI-based flexible polyurethane foam,” *Polym. Degrad. Stab.*, vol. 98, no. 2, pp. 535–541, Feb. 2013, doi: 10.1016/j.polymdegradstab.2012.12.002.
- [11] “CEMENT_ALL_Datasheet_DS_024_EN.pdf.” Accessed: Sept. 17, 2025. [Online]. Available: https://www.ctscement.com/assets/doc/datasheets/CEMENT_ALL_Datasheet_DS_024_EN.pdf
- [12] “Standard Test Methods for Measuring Adhesion by Tape Test.” Accessed: Aug. 29, 2025. [Online]. Available: <https://store.astm.org/d3359-09.html>
- [13] Franklin Associates, A Division of ERG, “Cradle-to-Gate Life Cycle Analysis of Polyether Polyol for Flexible Foam Polyurethanes,” pp. 1–67, Dec. 2022.

Appendix

Appendix A: Particle Size Distribution

Figure A1 shows the distribution for particle size of both processing conditions. For foam powder processed under CO₂, the average size is 0.176 mm, while the median is 0.169 mm. For foam powder processed under N₂, the average size is 0.166 mm, while the median is 0.162 mm. In both cases, the median is less than the mean, indicating a slight right-skew for both conditions.

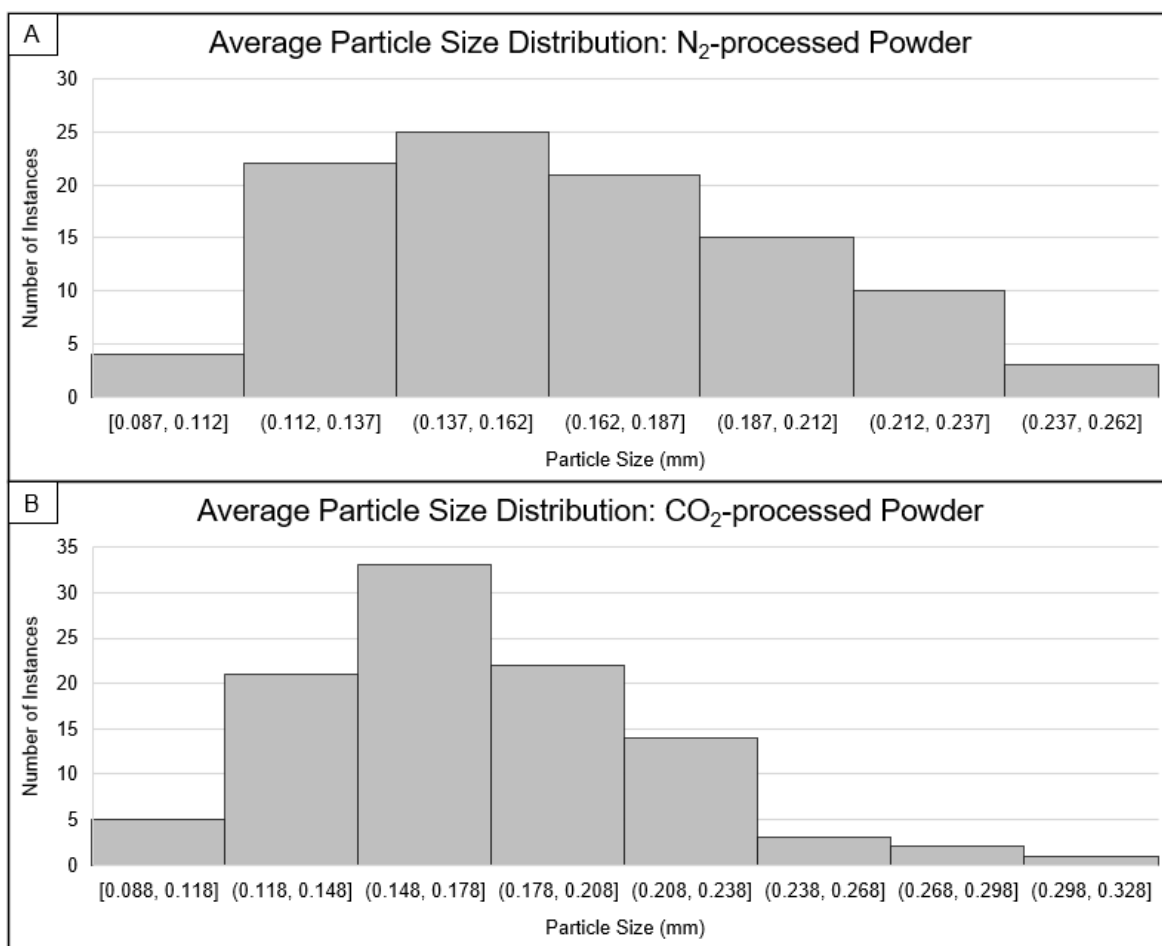


Figure A1: Particle Size Distribution of Foam Powder. (A) shows distribution for N₂-processed powder, while (B) shows distribution for CO₂-processed powder. Both histograms indicate a slight right-skew in the data.

Appendix B: Density Measurements for Cement Samples with Foam Powder Additive

Table B1 shows all measurements taken to determine average densities of cement samples with foam powder additive.



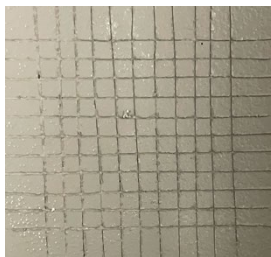
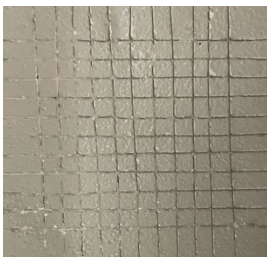
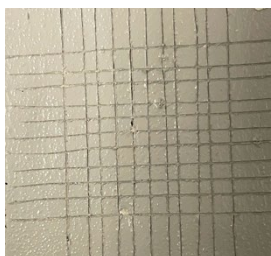



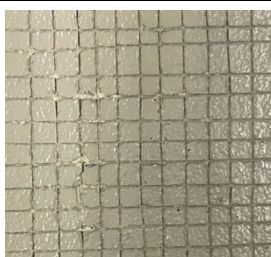

Table B1: Average Density across Cement Samples with Foam Additive

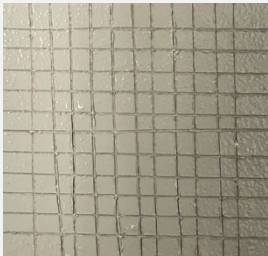

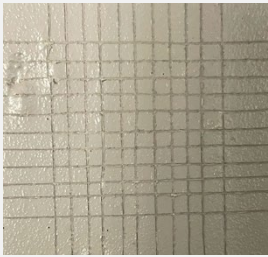
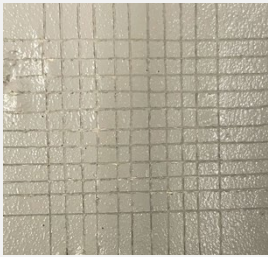




Condition		Mass (g)			Dimensions (cm)						Density (g/cc)			
		Rep. 1	Rep. 2	Avg.		W	L	H	Vol.	Avg.	Rep. 1	Rep. 2	Avg.	SE
Negative Control		182.89	162.01	172.45	Rep 1	5.625	8.176	2.05	94.28	87.45	1.94	2.01	1.97	0.035
					Rep 2	5.53	8.154	1.788	80.62					
CO ₂	5%	167.03	172.41	169.72	Rep 1	5.595	8.133	1.881	85.59	87.12	1.95	1.95	1.95	0.003
					Rep 2	5.639	8.17	1.924	88.64					
	10%	155.21	162.4	158.81	Rep 1	5.582	8.14	1.815	82.47	84.97	1.88	1.86	1.87	0.013
					Rep 2	5.59	8.167	1.916	87.47					
	15%	154.87	162.31	158.59	Rep 1	5.559	8.148	1.828	82.80	84.07	1.87	1.90	1.89	0.016
					Rep 2	5.533	8.195	1.882	85.34					
	20%	151.99	153.83	152.91	Rep 1	5.52	8.155	1.87	84.18	83.67	1.81	1.85	1.83	0.022
					Rep 2	5.557	8.192	1.827	83.17					
N ₂	5%	176.98	166.19	171.59	Rep 1	5.621	8.147	2.025	92.73	88.81	1.91	1.96	1.93	0.025
					Rep 2	5.507	8.177	1.885	84.88					
	10%	163.87	151.6	157.74	Rep 1	5.628	8.186	1.861	85.74	82.57	1.91	1.91	1.91	0.001
					Rep 2	5.487	8.175	1.77	79.40					
	15%	154.07	163.34	158.71	Rep 1	5.502	8.067	1.818	80.69	84.25	1.91	1.86	1.88	0.025
					Rep 2	5.547	8.198	1.931	87.81					
	20%	148.86	142.83	145.85	Rep 1	5.635	8.061	1.836	83.40	83.17	1.78	1.72	1.75	0.031
					Rep 2	5.575	8.09	1.839	82.94					

Appendix C: Paint Peel Test Comparison Images

Table C1 shows all before and after images taken to analyze paint adhesion to cement samples with foam powder additive.

Table C1. Paint Peel Test Rating Images

Condition		Before	After	Rating
Negative Control				3B
CO ₂	5%			4B
	10%			3B
	15%			4B
	20%			3B

N ₂	5%			3B
	10%			4B
	15%			4B
	20%			4B

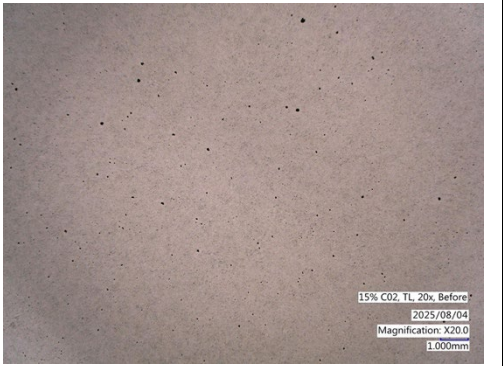

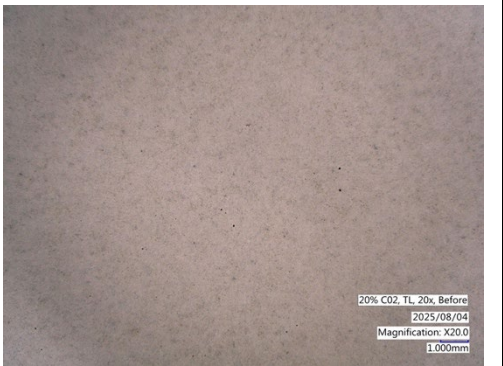

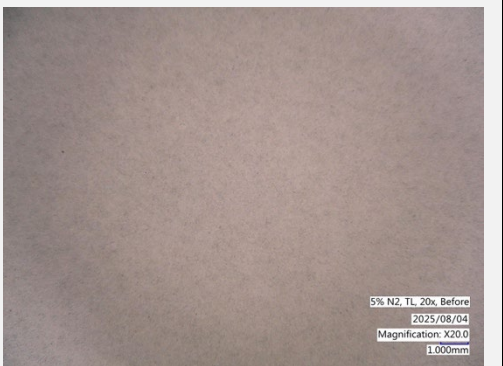
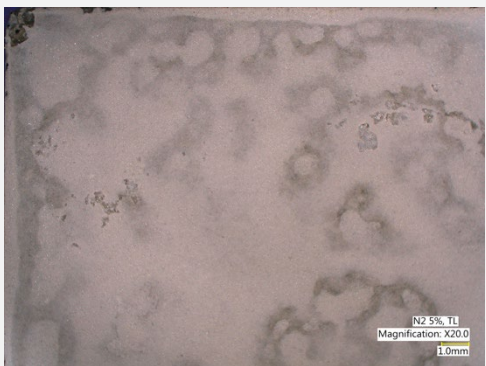
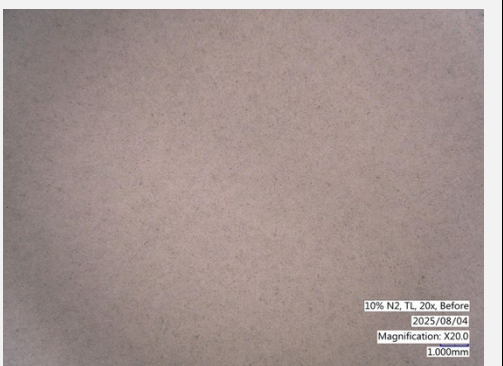

Appendix D: Salt Spray Exposure Comparison Images

Tables D1-5 shows all before and after images taken of each corner and center locations on each cement sample that underwent salt spray exposure for one week.

Table D1. Salt Exposure Images – Top Left

Condition		Before	After
Negative Control			
CO ₂	5%		
	10%		

Converting Post-Consumer Recycled Polyurethane Mattress Foam into Surface-engineered Powders
Final Report (Contains no confidential information)

	15%	 <p>15% CO2, TL, 20x, Before 2025/08/04 Magnification: X20.0 1.000mm</p>	 <p>CO2 15%, TL Magnification: X20.0 1.0mm</p>
	20%	 <p>20% CO2, TL, 20x, Before 2025/08/04 Magnification: X20.0 1.000mm</p>	 <p>CO2 20%, TL Magnification: X20.0 1.0mm</p>
N ₂	5%	 <p>5% N2, TL, 20x, Before 2025/08/04 Magnification: X20.0 1.000mm</p>	 <p>N2 5%, TL Magnification: X20.0 1.0mm</p>
	10%	 <p>10% N2, TL, 20x, Before 2025/08/04 Magnification: X20.0 1.000mm</p>	 <p>N2 10%, TL Magnification: X20.0 1.0mm</p>


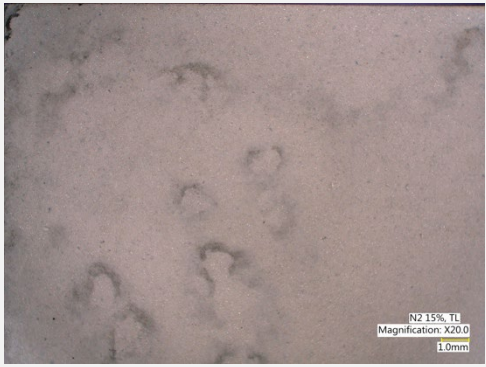
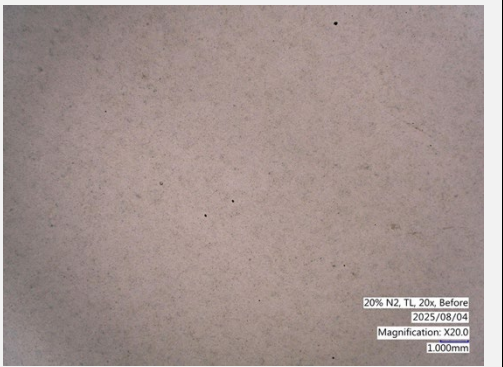


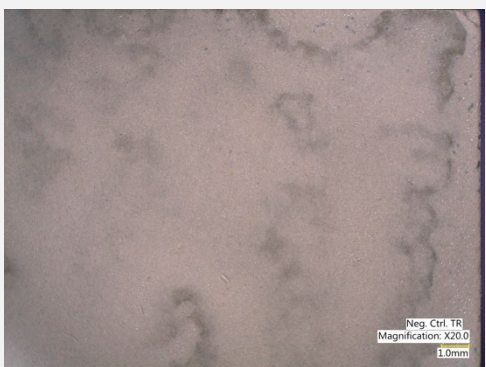
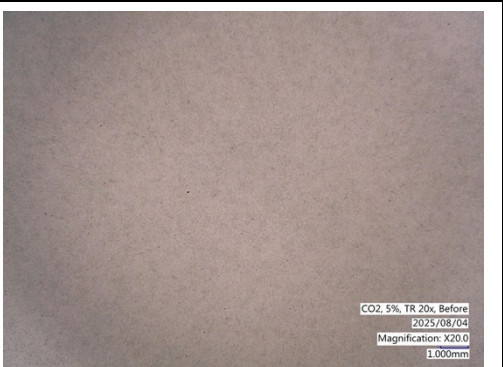

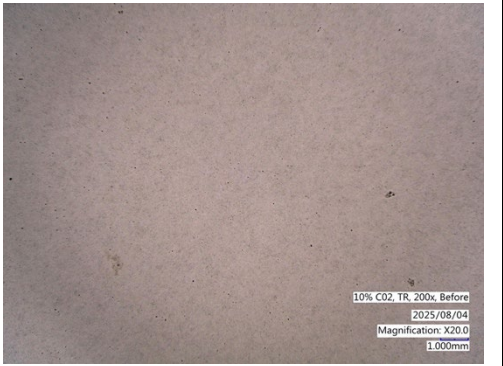
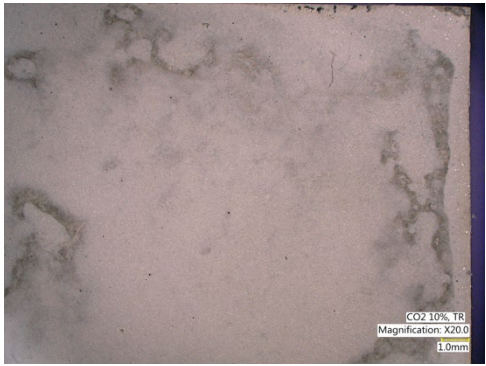
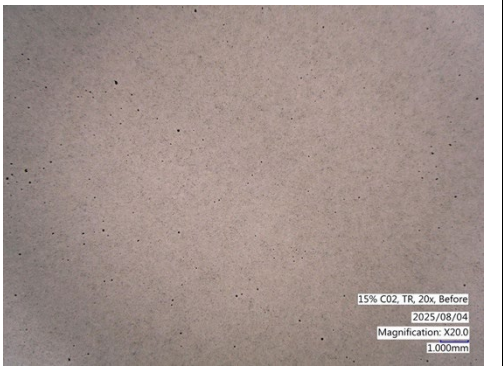

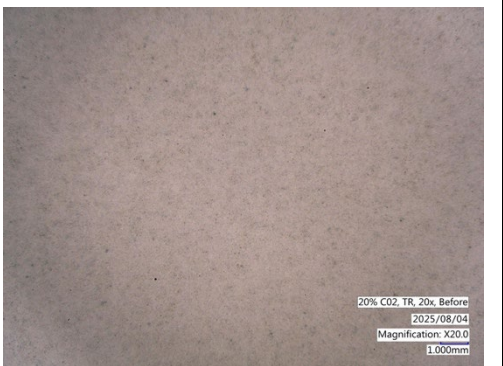

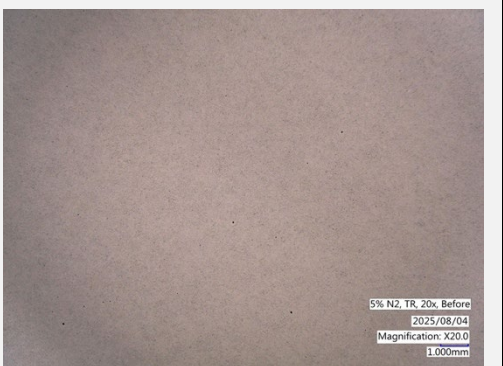

	15%		
	20%		

Table D2. Salt Exposure Images – Top Right

Condition		Before	After
Negative Control			
CO ₂	5%		

Converting Post-Consumer Recycled Polyurethane Mattress Foam into Surface-engineered Powders
Final Report (Contains no confidential information)

	10%	 <p>10% CO2, TR, 200x, Before 2025/08/04 Magnification: X20.0 1.000mm</p>	 <p>CO2 10%, TR Magnification: X20.0 1.0mm</p>
	15%	 <p>15% CO2, TR, 20x, Before 2025/08/04 Magnification: X20.0 1.000mm</p>	 <p>CO2 15%, TR Magnification: X20.0 1.0mm</p>
	20%	 <p>20% CO2, TR, 20x, Before 2025/08/04 Magnification: X20.0 1.000mm</p>	 <p>CO2 20%, TR Magnification: X20.0 1.0mm</p>
N ₂	5%	 <p>5% N2, TR, 20x, Before 2025/08/04 Magnification: X20.0 1.000mm</p>	 <p>N2 5%, TR Magnification: X20.0 1.0mm</p>

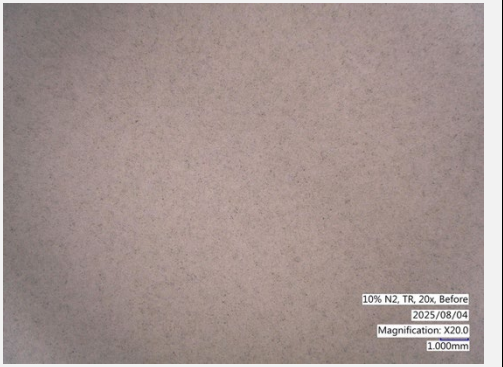


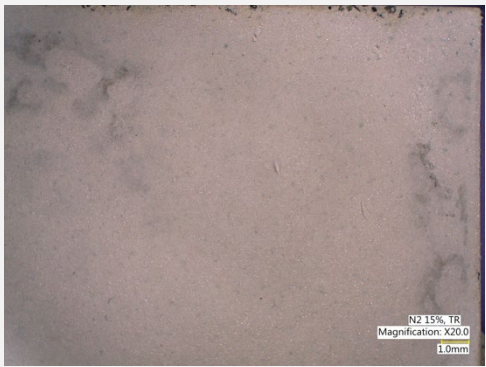


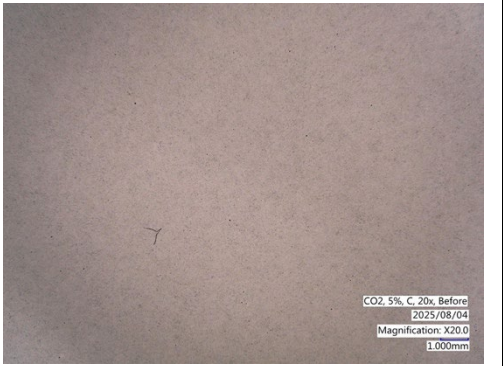

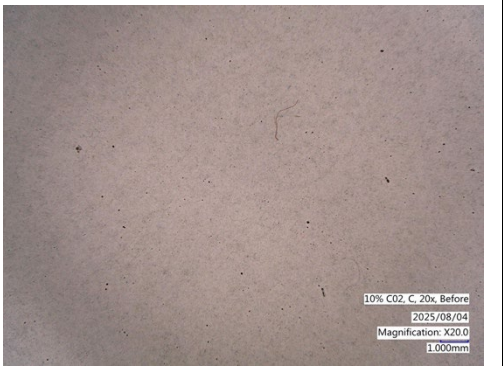
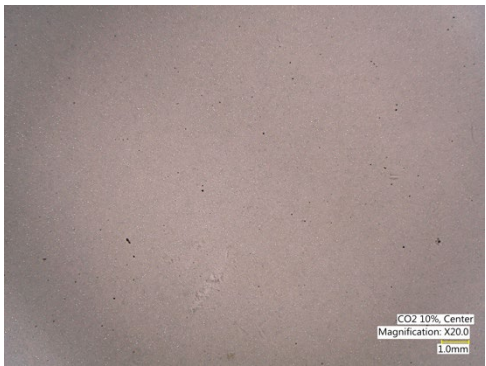
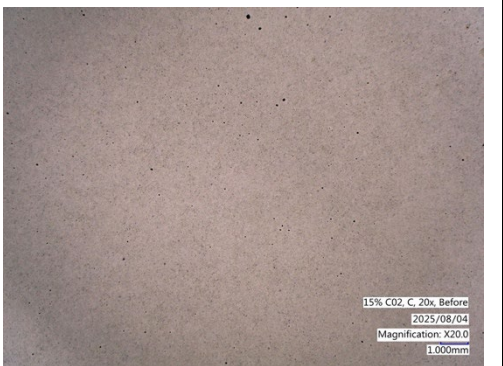
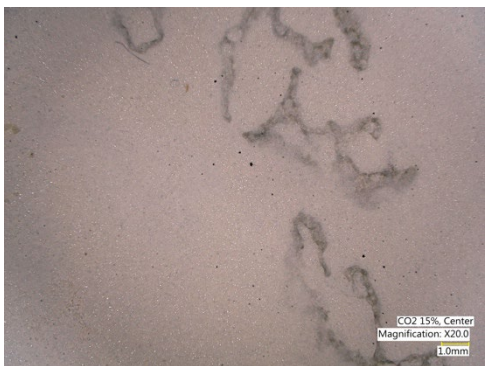
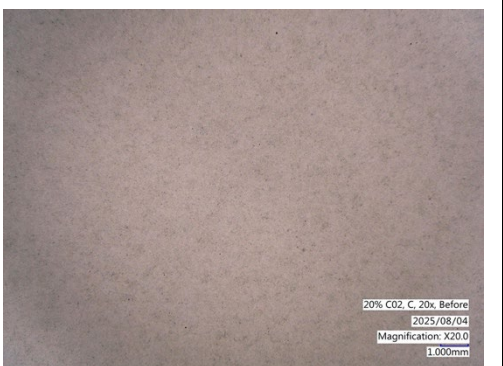

	10%	 <p>10% N2, TR, 20x, Before 2025/08/04 Magnification: X20.0 1.000mm</p>	 <p>N2 10%, TR Magnification: X20.0 1.0mm</p>
	15%	 <p>15% N2, TR, 20x, Before 2025/08/04 Magnification: X20.0 1.000mm</p>	 <p>N2 15%, TR Magnification: X20.0 1.0mm</p>
	20%	 <p>20% N2, TR, 20x, Before 2025/08/04 Magnification: X20.0 1.000mm</p>	 <p>N2 20%, TR Magnification: X20.0 1.0mm</p>

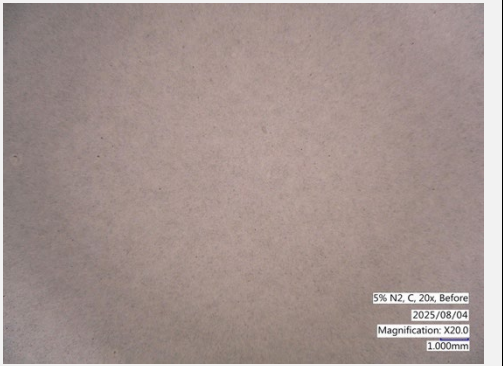
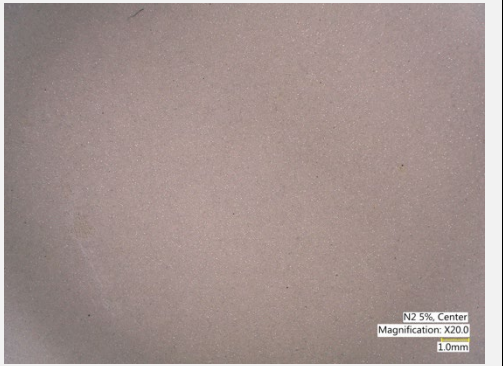
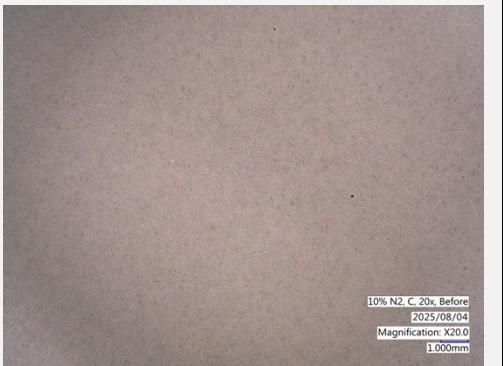
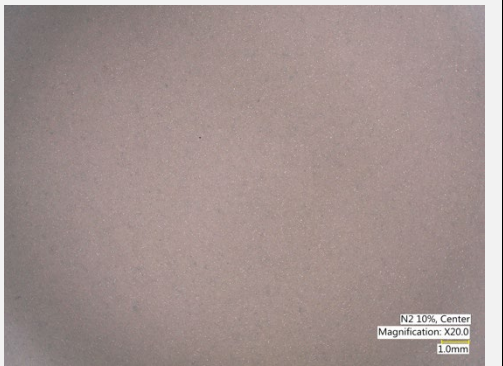
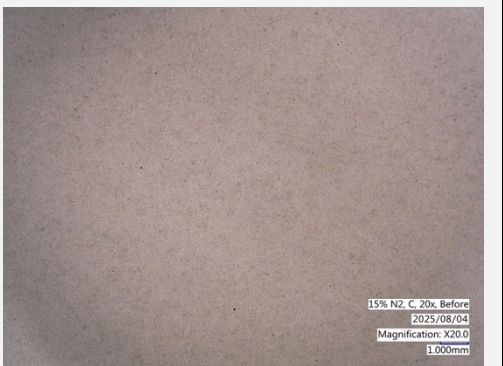

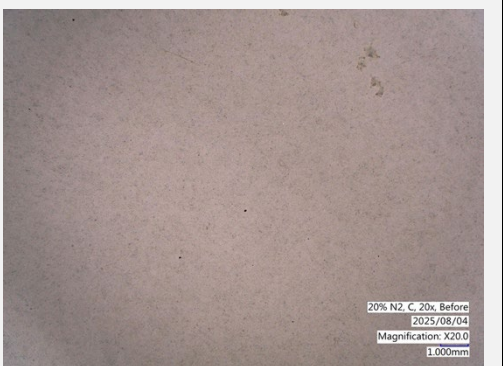

Table D3. Salt Exposure Images – Center

Condition	Before	After
Negative Control	 <p>-ctrl, C, 20x, before 2025/08/04 Magnification: X20.0 1.000mm</p>	 <p>Neg. Ctrl. Center Magnification: X20.0 1.0mm</p>

Converting Post-Consumer Recycled Polyurethane Mattress Foam into Surface-engineered Powders
Final Report (Contains no confidential information)


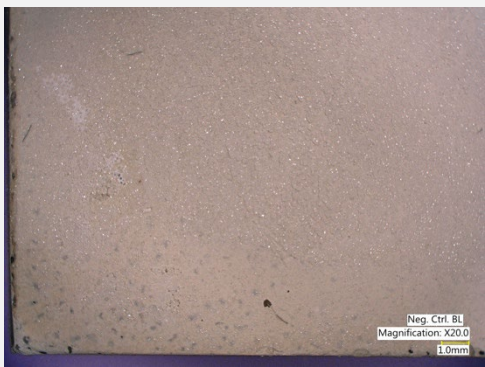
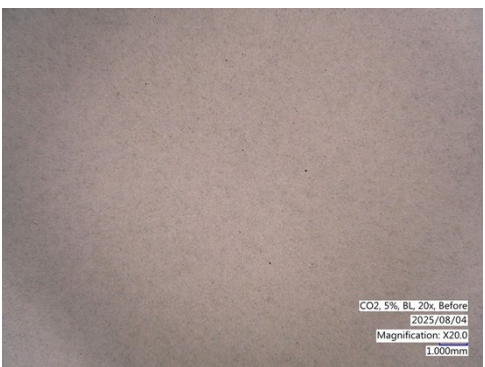
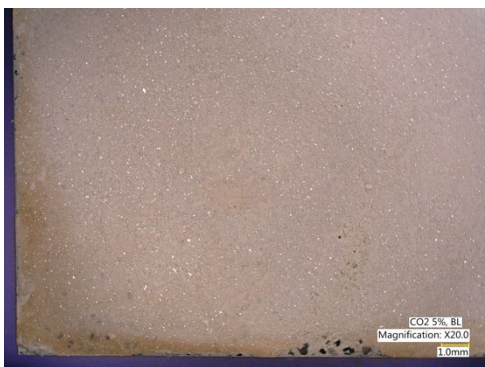




CO ₂	5%	 <p>CO2, 5%, C, 20x, Before 2025/08/04 Magnification: X20.0 1.000mm</p>	 <p>CO2 5%, Center Magnification: X20.0 1.0mm</p>
	10%	 <p>10% CO2, C, 20x, Before 2025/08/04 Magnification: X20.0 1.000mm</p>	 <p>CO2 10%, Center Magnification: X20.0 1.0mm</p>
	15%	 <p>15% CO2, C, 20x, Before 2025/08/04 Magnification: X20.0 1.000mm</p>	 <p>CO2 15%, Center Magnification: X20.0 1.0mm</p>
	20%	 <p>20% CO2, C, 20x, Before 2025/08/04 Magnification: X20.0 1.000mm</p>	 <p>CO2 20%, Center Magnification: X20.0 1.0mm</p>

Converting Post-Consumer Recycled Polyurethane Mattress Foam into Surface-engineered Powders
Final Report (Contains no confidential information)

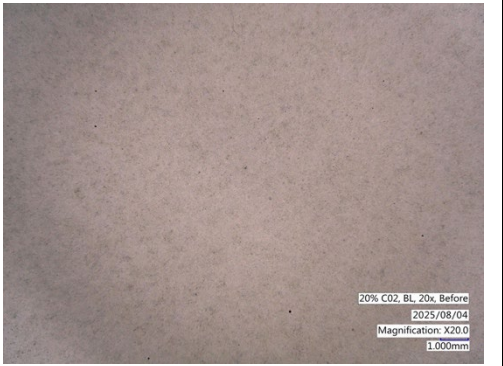
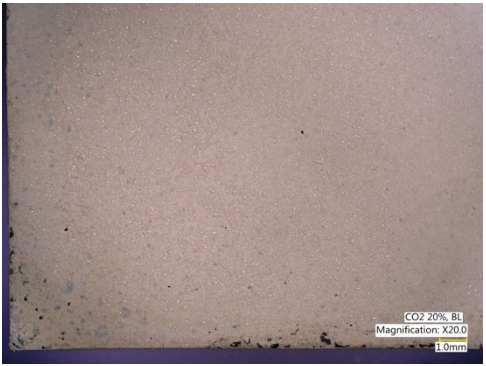
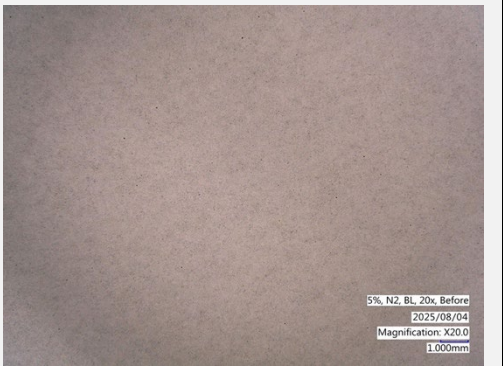
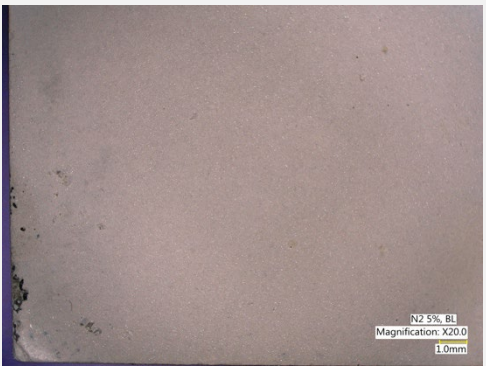
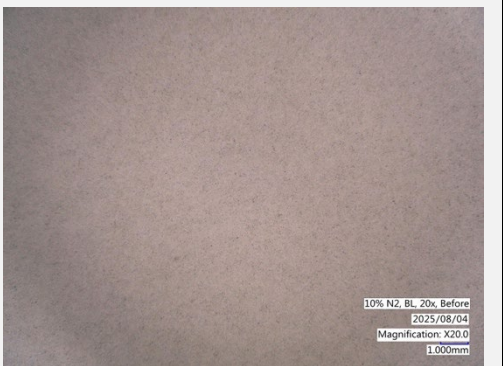
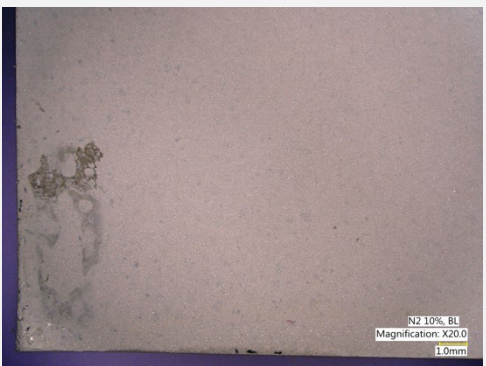

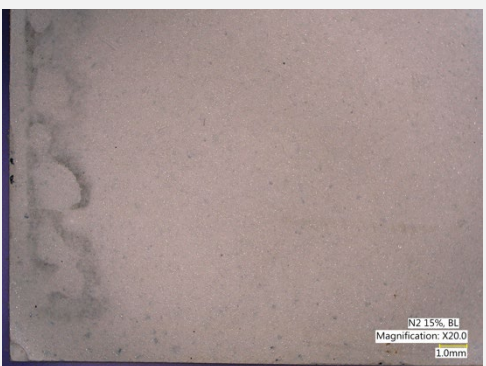
N ₂	5%	 <p>5% N2, C, 20x, Before 2025/08/04 Magnification: X20.0 1.000mm</p>	 <p>N2 5%, Center Magnification: X20.0 1.0mm</p>
	10%	 <p>10% N2, C, 20x, Before 2025/08/04 Magnification: X20.0 1.000mm</p>	 <p>N2 10%, Center Magnification: X20.0 1.0mm</p>
	15%	 <p>15% N2, C, 20x, Before 2025/08/04 Magnification: X20.0 1.000mm</p>	 <p>N2 15%, Center Magnification: X20.0 1.0mm</p>
	20%	 <p>20% N2, C, 20x, Before 2025/08/04 Magnification: X20.0 1.000mm</p>	 <p>N2 20%, Center Magnification: X20.0 1.0mm</p>

Converting Post-Consumer Recycled Polyurethane Mattress Foam into Surface-engineered Powders
Final Report (Contains no confidential information)

Table D4. Salt Exposure Images – Bottom Left

Condition		Before	After
Negative Control			
CO ₂	5%		
	10%		
	15%		

Converting Post-Consumer Recycled Polyurethane Mattress Foam into Surface-engineered Powders
Final Report (Contains no confidential information)

	20%		
N ₂	5%		
	10%		
	15%		

Converting Post-Consumer Recycled Polyurethane Mattress Foam into Surface-engineered Powders
Final Report (Contains no confidential information)


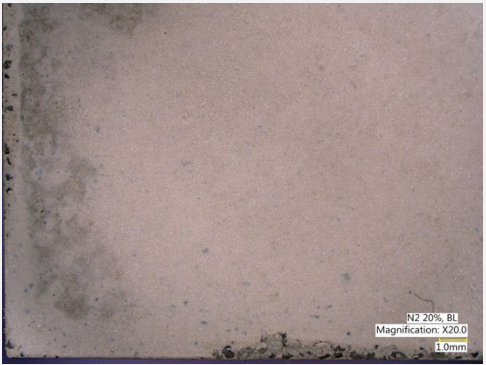
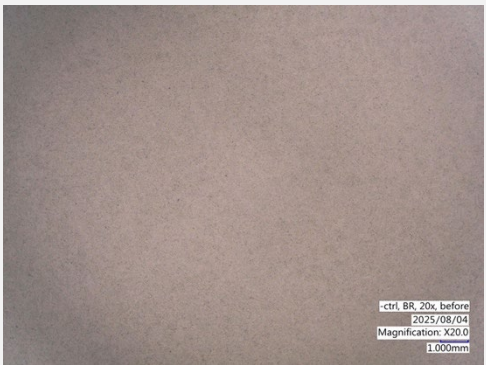
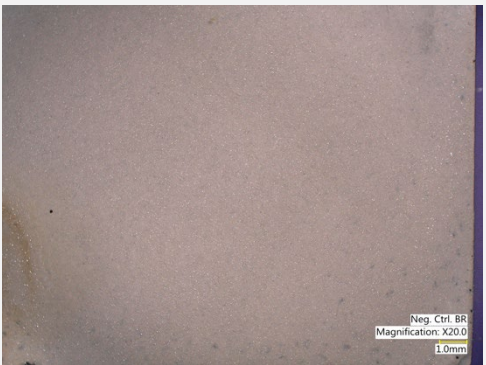


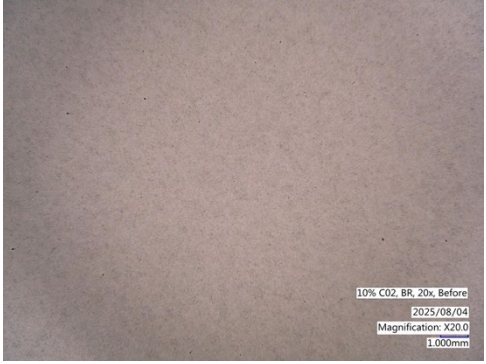

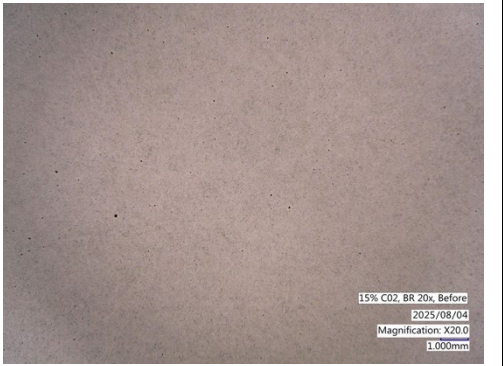



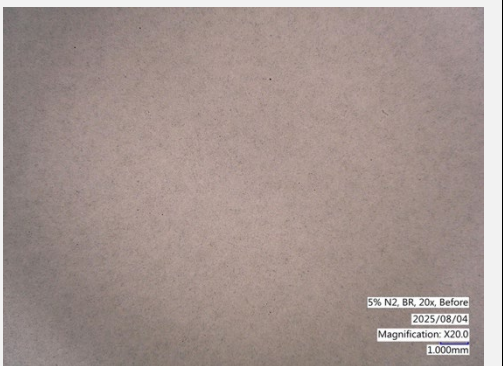

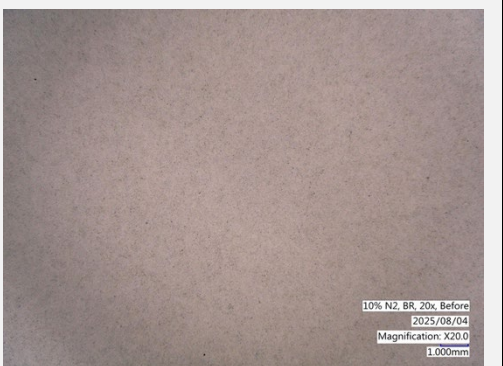

	20%		
--	-----	---	--

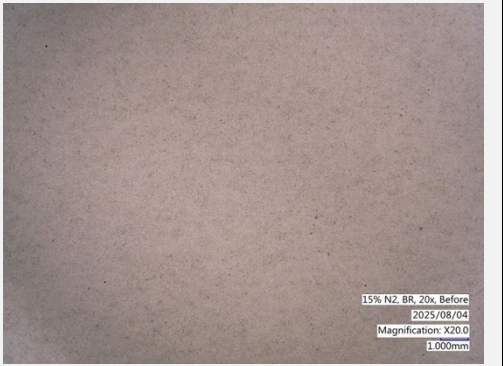

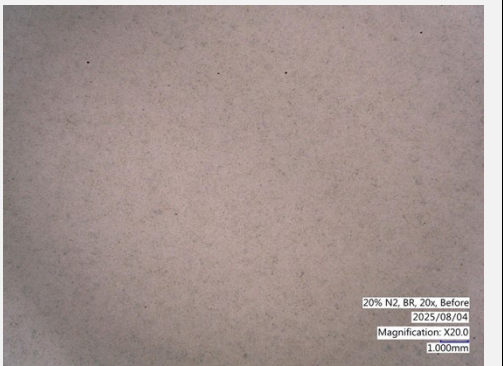

Table D5. Salt Exposure Images – Bottom Right

Condition		Before	After
Negative Control			
CO ₂	5%		
	10%		

Converting Post-Consumer Recycled Polyurethane Mattress Foam into Surface-engineered Powders
Final Report (Contains no confidential information)

	15%	 <p>15% CO2 BR 20x Before 2025/08/04 Magnification: X20.0 1.000mm</p>	 <p>CO2 15% BR Magnification: X20.0 1.0mm</p>
	20%	 <p>20% CO2 BR 20x Before 2025/08/04 Magnification: X20.0 1.000mm</p>	 <p>CO2 20% BR Magnification: X20.0 1.0mm</p>
N ₂	5%	 <p>5% N2 BR 20x Before 2025/08/04 Magnification: X20.0 1.000mm</p>	 <p>N2 5% BR Magnification: X20.0 1.0mm</p>
	10%	 <p>10% N2 BR 20x Before 2025/08/04 Magnification: X20.0 1.000mm</p>	 <p>N2 10% BR Magnification: X20.0 1.0mm</p>

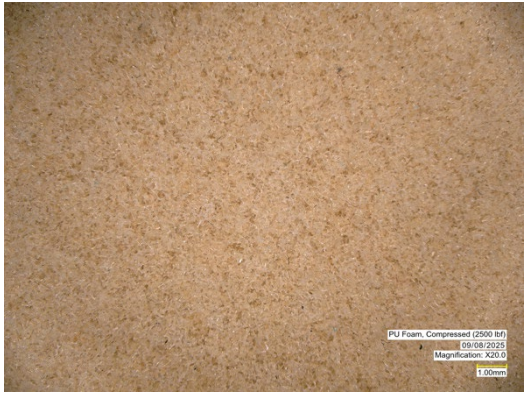
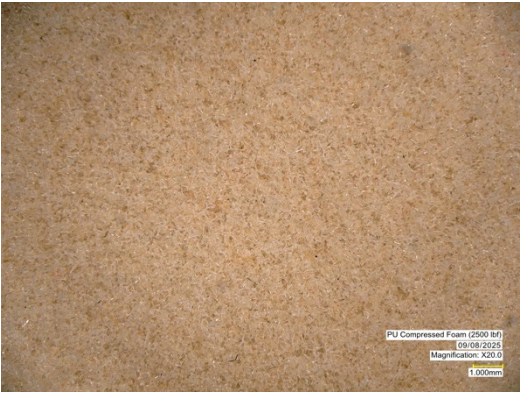

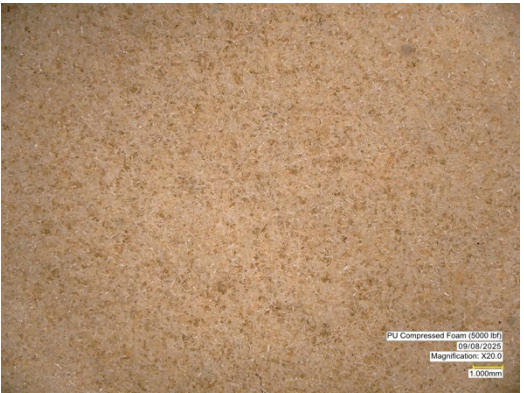


Converting Post-Consumer Recycled Polyurethane Mattress Foam into Surface-engineered Powders
Final Report (Contains no confidential information)

	15%	 <p>15% N2, BR, 20x, Before 2025/08/04 Magnification: X20.0 1.000mm</p>	 <p>N2 15%, BR Magnification: X20.0 1.0mm</p>
	20%	 <p>20% N2, BR, 20x, Before 2025/08/04 Magnification: X20.0 1.000mm</p>	 <p>N2 20%, BR Magnification: X20.0 1.0mm</p>

Appendix E: Compressed Foam Sheets

Tables E1-3 show all compressed sheets microscopically.

Table E1. Compressed Foam Sheets (20x)

Compressive Force (lbf)	N ₂	CO ₂
2.5k		
5k		
10k		

Converting Post-Consumer Recycled Polyurethane Mattress Foam into Surface-engineered Powders
Final Report (Contains no confidential information)


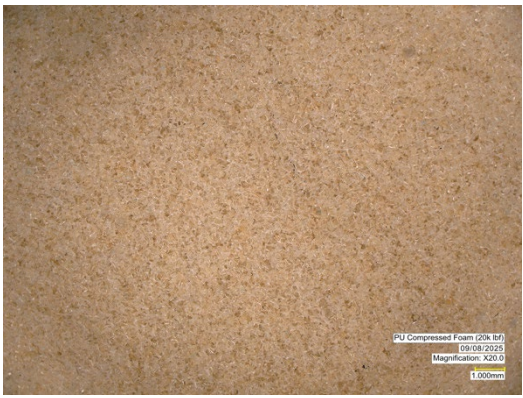
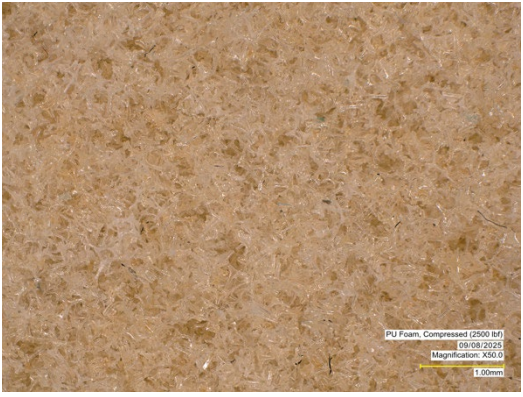
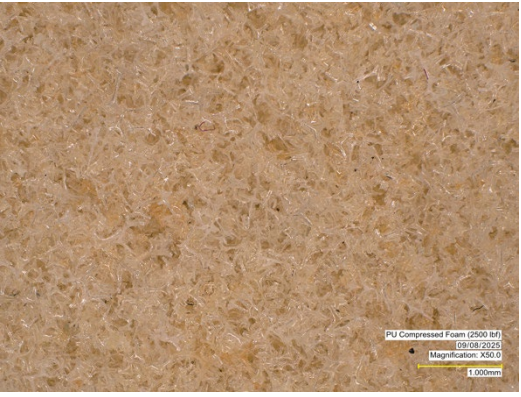
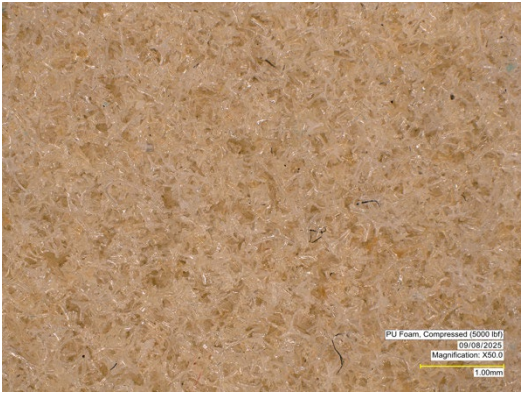
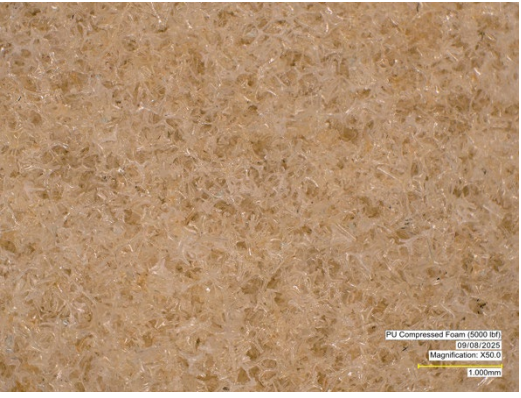
20k		
-----	---	--

Table E2. Compressed Foam Sheets (50x)

Compressive Force (lb.)	N ₂	CO ₂
2.5k		
5k		

Converting Post-Consumer Recycled Polyurethane Mattress Foam into Surface-engineered Powders
Final Report (Contains no confidential information)


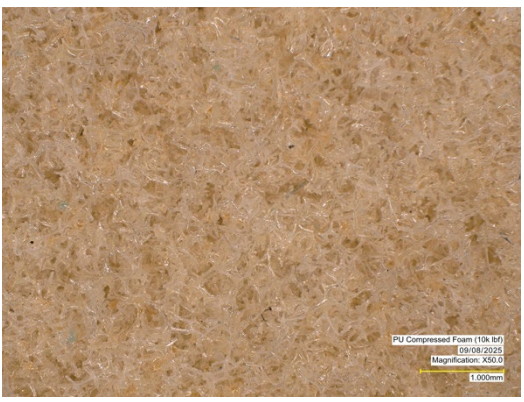
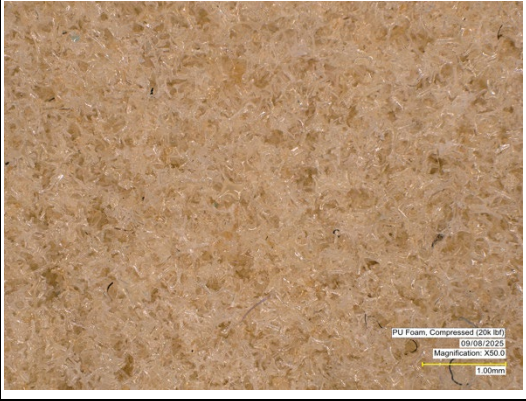



10k	 <p>PU Foam, Compressed (10k lbf) 09/08/2025 Magnification: X20.0 1.00mm</p>	 <p>PU Compressed Foam (10k lbf) 09/08/2025 Magnification: X50.0 1.00mm</p>
20k	 <p>PU Foam, Compressed (20k lbf) 09/08/2025 Magnification: X20.0 1.00mm</p>	 <p>PU Compressed Foam (20k lbf) 09/08/2025 Magnification: X50.0 1.00mm</p>

Table E3. Compressed Foam Sheets (20k lab, 2 min. dwell time)

20x	50x
 <p>PU Compressed Foam (20k lbf, 2 min dwell time) 09/08/2025 Magnification: X20.0 1.00mm</p>	 <p>PU Compressed Foam (20k lbf, 2 min dwell time) 09/08/2025 Magnification: X50.0 1.00mm</p>